International Journal of Cognitive Computing in Engineering 5 (2024) 27–43

Contents lists available at ScienceDirect

International Journal of Cognitive Computing in Engineering

journal homepage: www.keaipublishing.com/en/journals/international-journal-of-cognitive-computing-in-engineering/

Exploring static rebalancing strategies for dockless bicycle sharing systems based on multi-granularity behavioral decision-making

Chao Zhang [a,b,*], Jiahui Zhang [a], Wentao Li [c,a], Oscar Castillo [d], Jiayi Zhang [e]

[a] School of Computer and Information Technology, Shanxi University, Taiyuan, 030006, China
[b] Key Laboratory of Computational Intelligence and Chinese Information Processing of Ministry of Education, Shanxi University, Taiyuan 030006, China
[c] College of Artificial Intelligence, Southwest University, Chongqing, 400715, China
[d] Division of Graduate Studies and Research, Tijuana Institute of Technology, Tijuana, 22379, Mexico
[e] School of Computer Science and Statistics, Trinity College Dublin, Dublin 2, Ireland

ARTICLE INFO

Keywords:
Urban dockless bicycle sharing system
Modern intelligent transportation systems
Multi-granularity
Complex intuitionistic fuzzy set
Prospect-regret theory

ABSTRACT

In the continuously evolving context of urbanization, more people flock to cities for job opportunities and an improved quality of life, resulting in undeniable pressure on transportation networks. This leads to severe daily commuting challenges for residents. To mitigate this urban traffic pressure, most cities have adopted urban dockless bicycle sharing systems (UDBSS) as an effective measure. However, making accurate decisions regarding UDBSS demand in different city locations is crucial, as incorrect choices can worsen transportation problems, causing difficulties in finding bicycles or excessive deployments leading to disorderly accumulation. To address this decision-making challenge, it is essential to consider uncertain factors like daily weather, temperature, and workdays. To tackle this effectively, we construct an adjustable multi-granularity (MG) complex intuitionistic fuzzy (CIF) information system using complex intuitionistic fuzzy sets (CIFSs). This system objectively determines classification thresholds using an evaluation-based three-way decision (TWD) method, creating adjustable MG CIF probabilistic rough sets (PRSs). Additionally, to recognize the irrationality of decision-makers (DMs), we propose a method that combines prospect theory (PT) with regret theory (RT), providing a more comprehensive understanding of the influence of DMs' psychological factors on decision outcomes. Building upon these foundations, we present static rebalancing strategies for UDBSS based on MG PRSs and prospect-regret theory (P-RT) within the CIF information system. Finally, using UDBSS data collected from various sensors, we conduct experimental analysis to verify its feasibility and stability. In summary, this approach considers residents' daily usage preferences, including bicycles utilization and return, with the aim of minimizing unmet resident demands and predicting usage patterns for the next day. It effectively addresses the issue of UDBSS distribution inefficiencies and holds a significant advantage in prediction, making it suitable for broader applications in transportation systems and contributing to the establishment of more advanced modern intelligent transportation systems (MITSs) in the future.

1. Introduction

In recent decades, as the process of urbanization has accelerated, a significant population has been congregating in cities, bringing about escalating issues such as traffic congestion. Faced with this challenge, the sharing economy has become one of the topics that people eagerly discuss, and it cannot be ignored. Taking UDBSS as an example, this exemplifies the sharing economy and stands out amidst numerous discussions. UDBSS, in a unique manner facilitated by large-scale deployment (Gao et al., 2023). In China, UDBSS has already expanded to cover

This paper was supported by the National Natural Science Foundation of China (62272284; 12201518; 62072294; 61972238), the Special Fund for Science and Technology Innovation Teams of Shanxi (202204051001015), the China Postdoctoral Science Foundation (No. 2023T160401), the Natural Science Foundation of Chongqing (No. CSTB2023NSCQ-MSX0152), the Science and Technology Research Program of Chongqing Education Commission (KJQN202300202; KJQN202100205; KJQN202100206), the Training Program for Young Scientific Researchers of Higher Education Institutions in Shanxi, and the Cultivate Scientific Research Excellence Programs of Higher Education Institutions in Shanxi (CSREP) (2019SK036).

* Corresponding author: School of Computer and Information Technology, Shanxi University, Taiyuan, 030006, China.
E-mail address: czhang@sxu.edu.cn (C. Zhang).

https://doi.org/10.1016/j.ijcce.2024.01.001
Received 5 November 2023; Received in revised form 3 December 2023; Accepted 1 January 2024
Available online 2 January 2024

over 360 cities, with an average daily travel distance of 47 million kilometers. Consequently, after their introduction, the congestion delay index has, on average, decreased by 2.2 %, with a more pronounced effect on weekdays compared to weekends (Huang and Xu, 2023). This approach not only reduces the personal demand for private bicycles, easing traffic congestion and enhancing urban traffic flow, but also greatly mitigates energy waste and the environmental pollution caused by discarded bicycles (Zhang and Mi, 2018). These UDBSS provides city residents with an efficient and eco-friendly transportation choice, setting them apart within the modern transportation framework. Therefore, they have emerged as an emerging and crucial mode of transportation in the contemporary transport landscape (Gu et al., 2019).

As mentioned above, for UDBSS in modern transportation to unlock their substantial potential and effectively alleviate issues such as traffic congestion, they need to possess the features of multi-location and multi-quantity deployment within cities. The most fundamental requirement is that, in most cases, residents should not encounter difficulties in using bicycles, and there should be minimal resource wastage, aiming for a state of equilibrium as much as possible (Ramachandran and Sangaiah, 2021).

When UDBSS was initially introduced, some city administrators addressed this requirement by deploying a significant number of bicycles across various areas within the city, yielding notable outcomes. However, it's clear that this approach leads to another serious concern, namely the overabundance of idle bicycles in areas with lower foot traffic. This results in haphazard accumulation of UDBSS and the squandering of substantial available resources. It is apparent that this practice contradicts the initial purpose of the sharing economy in mitigating traffic congestion (Ramachandran and Sangaiah, 2021; Wang et al., 2021). On the other hand, some policymakers exclusively focus on deploying bicycles in key urban zones, overlooking residential and industrial areas, and consequently failing to meet the commuting needs of many residents, which almost prevents them from fully harnessing the potential of the sharing economy. Obviously, the traditional method cannot reasonably distribute the shared bicycles in each station to meet the needs of residents to the greatest extent, that is, it cannot restore the unbalanced UDBSS to a balanced state.

In conclusion, to harness the full potential of urban shared bicycles within MITSs, the key lies in finding innovative approaches to strike a balance between deployment diversity and distribution equity, with the aim of minimizing unmet travel demands of residents. We believe that a viable strategy is the implementation of an intelligent scheduling system. This system would dynamically adjust the deployment of shared bicycles at various times and locations based on collected data and predictive models, ensuring a more rational and equitable distribution of vehicles.

Currently, with the ongoing progress of the third revolution in the information technology industry, the role of the Internet of Things (IoT) in the field of transportation is becoming increasingly significant, providing a tangible foundation for building smart cities. Furthermore, it can be recognized that the MITSs serves as a perfect example of services supporting smart cities (Sathiyaprasad, 2023; Gokasar et al., 2023; Deveci et al., 2023). Leveraging the data collection and high-speed transmission capabilities of the IoT, a vast MITSs is rapidly emerging. In this evolving MITSs, various sensors are not only capable of real-time data collection and processing with corresponding feedback but also capable of storing this data, creating an extensive database encompassing diverse types of information. These data provide crucial real-world foundations for subsequent research, experiments, and learning (Bilotta and Nesi, 2022). Zhao et al. (2023) used 6G technology, integrated sensing and communication, to improve the stability of the vehicle's interaction with information from the surrounding scene. Thinh et al. (2023) built an IoT system that can collect the operation data of transformers in unmanned substations from multiple perspectives to determine whether the current transformer is normal.

With the assistance of MITSs, we can collect, transmit, and store data using sensors and analyze past data to propose practical solutions to the issues mentioned earlier in the UDBSS field (Wang and Ma, 2022). For instance, Maleki et al. (2023) established a simulation system and utilized supervised learning methods to train models on a large set of generated bike-sharing rebalancing plans, aiming to achieve the optimal machine learning model as the final objective function. Qiao et al. (2023) first investigated how various factors influenced the quality of the final solution and then employed heuristic algorithms to address the shared bicycle rebalancing problem. In summary, with the help of IoT technology and data analysis, we can not only address the issue of unreasonable allocation in the urban bike-sharing sector but also gain insights into the dynamics of urban populations and urban structures. All of these contribute to providing essential insights for the development of a more intelligent and efficient MITSs (Xu et al., 2023).

In this context, we first achieve precise bike localization through positioning devices, recording the pickup and drop-off locations, as well as the corresponding timestamps for bikes used over multiple days. Due to the numerous uncertain factors affecting bike usage patterns (Eren and Uz, 2020), this problem can be viewed as an MG decision-making issue in a fuzzy environment. To overcome the limitations of individual DM in terms of knowledge, experience, and cognitive abilities, as well as to incorporate the bounded rationality of DMs, this paper employs an MG group decision-making (GDM) method that integrates PT and RT. In this scheme, the key focus is on applying a rational and effective MG GDM method to divide and analyze bike usage patterns at different granular levels based on the collected data, thus revealing potential patterns and trends.

Based on the description above, in order to accomplish the equitable allocation of shared bicycles, we have devised an adjustable MG GDM method based on a CIF information system, taking into account DMs' bounded rationality. Furthermore, we develop static rebalancing strategies for UDBSS with the goal of minimizing unmet resident demands. Below, we summarize the primary research motivations of this paper.

(1) Most of existing MG GDM methods in CIF environments choose to use MG rough sets or aggregation methods to fuse different granularities to handle MG problems. This may result in extreme granularity selection result in the decision process, or the results may deviate significantly from the initial evaluation values after integrating different granularities. Therefore, it is necessary to propose an MG GDM method that allows DMs to freely choose different granularity.
(2) Among the two existing bounded rationality methods, PT tends to describe DMs' cautious attitude towards losses and aggressive attitude towards gains, emphasizing the impact of emotions on DMs, however it does not directly address the regret emotions that people may feel after decision. RT focuses on people's potential regret emotions in the future, focusing on avoiding regret, but not fully considering people's weighing between potential benefits and losses, leading to relatively conservative decisions. Therefore, combining the two methods, that is P-RT, can compensate for their respective shortcomings and make the decision results more in line with people's decision behavior in different contexts.
(3) Currently, regarding the static rebalancing problem of UDBSS, more literature (Bulhões et al., 2018; Tian et al., 2020; Zhang et al., 2020) tends to focus on path optimization, emphasizing cost minimization. However, there are few articles that pay closer attention to resident demands. As an industry that prioritizes serving users, emphasizing the user experience is even more critical. Therefore, setting the minimization of unfulfilled resident demands as the objective for the rebalancing problem for UDBSS is highly necessary.

Through the research motivation of this paper, we further introduce the main contributions of this paper.

(1) When addressing MG problems in CIF environments, we propose an adjustable MG CIF PRSs based on the TWD framework. This method expands the range of choices for DMs across different granularities and enhances the accuracy of decision outcomes.
(2) Combining prospect theory with regret theory, we put forward P-RT. In the decision process, let the DMs not only pay attention to the loss and gain, but also include the regret that may be generated by the decision result into the decision factor. This makes the bounded rationality of DMs better reflected in the decision result.
(3) This paper, based on residents' daily usage preferences, validated the proposed model using a real urban shared bicycle data set. Sensitivity analysis and comparative analysis were conducted to confirm the effectiveness and feasibility of the UDSBB rebalancing model with the goal of minimizing unfulfilled resident demands. This model can be extended to address related issues in current and future intelligent transportation systems, providing an effective means for solving prediction problems.

Based on the above description, we give the rough flow diagram of the rebalancing model for UDBSS, shown as Fig. 1.

The structure of this text is described below. The literature related to the methods used in this model and the rebalancing problem for UDBSS is reviewed in Section 2. In Section 3, some relevant knowledge used in the model of this paper are introduced. In Section 4, the adjustable MG CIF PRSs based on P-RT is proposed. Then, the application method of a rebalancing model for UDBSS based on MG PRSs and P-RT in CIF information system is introduced in detail in Section 5. On the basis of this model, a real UDBSS case (https://citibikenyc.com/system-data) is used for experiments, and the detailed experimental process is shown in Section 6. Finally, the application value and development prospect of this method in the field of MITSs and the future research direction are summarized.

2. Literature review

In the Section 2, we investigate the current research status of the methods used in this paper and the rebalancing problem for UDBSS, and briefly summarize their development and key work.

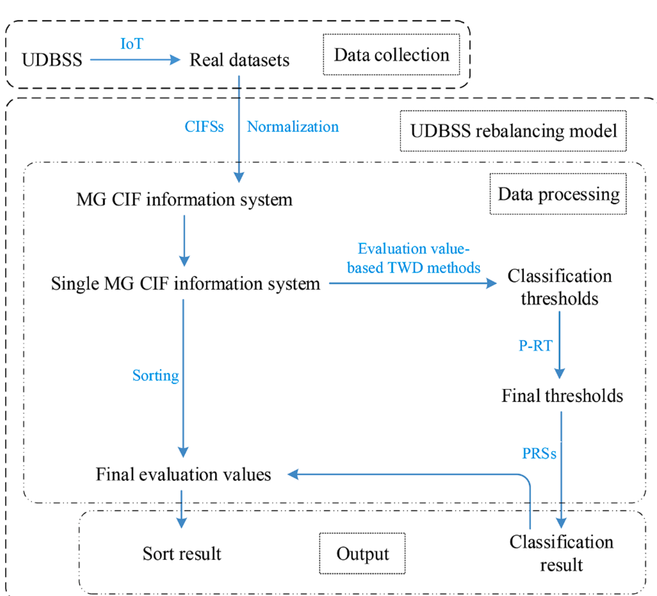

Fig. 1. The flow diagram of rebalancing model for UDBSS.

2.1. Introduction to CIFS

Decision-making plays a crucial role in various aspects of life, and most decision-making problems come with a significant amount of uncertain information. To effectively represent the fuzzy and uncertain information, Zadeh (1965) initiated the concept of fuzzy sets to represent this imprecise information in a fuzzy manner. However, as decision-making environments have become increasingly complex, classical fuzzy sets are no longer sufficient to fully and effectively describe various types of information. Consequently, a series of generalized fuzzy sets have emerged.

In 2010, Torra (2010) proposed the concept of hesitant fuzzy sets, which overcame difficulties in establishing membership degrees (MD). Atanassov (1986) introduced intuitionistic fuzzy sets (IFSs), which characterize information from both the MD and non-membership degrees (ND) perspectives. It requires that the sum of MD and ND is less than 1, which allows for the calculation of information uncertainty. Subsequently, Pythagorean fuzzy sets extended IFS, requiring that the sum of the squares of MD and ND be less than 1 (Hussain et al., 2020). Lin et al. (2021) proposed a new correlation coefficient to calculate the relationship between two Pythagorean fuzzy sets in view of the deficiency of the correlation coefficient between the existing PFSs. Lin et al. (2018), (2019) explored new clustering algorithms and edge computing of probabilistic linguistic term sets. In 2002, Ramot et al. (2002) introduced the concept of complex fuzzy sets (CFSs) to describe two-dimensional information more comprehensively. Complex fuzzy numbers (CFNs) consist of two variables r and ω that meet $0 < r < 1$ and $0 < \omega < 2\pi$. This allowed for the independent characterization of two features. To further enhance the capability of fuzzy sets in information representation, Alkouri and Salleh (2012) merged the two types of fuzzy sets mentioned above, providing various fundamental operations, giving rise to CIFSs.

This concept successfully inherits the advantages of IFS and CFS in information representation, enabling DMs to describe uncertain information more comprehensively, effectively improving the credibility and accuracy of decision results. Given the superiority of CIFSs in representing uncertain information, in recent years, they have found widespread application in various decision problems involving uncertainty. Researchers such as Garg and Rani (2019), (2020), (2020), 2019, (2017), (2020) have studied aggregation operator methods, distance measures, similarity measures, etc. about CIFSs and conducted relevant experiments. Wang (2022) in an incomplete CIF environment, proposed a missing value estimating algorithm to address the choice of various educational platforms during a pandemic and developed a GDM algorithm accordingly. Akram et al., 2021) presented a CIF multi-attribute decision-making model to determine the optimal power source.

In summary, CIFSs provide DMs with more flexible and comprehensive tools, particularly effective in addressing decision problems involving two-dimensional information and high uncertainty. Therefore, using CIFSs as the fuzzy environment in this paper is highly appropriate.

2.2. Introduction to the MG TWD method

When individuals face decision-making problems, the complexity of the decision-making environment mainly arises from the inclusion of numerous influencing factors. In such cases, using decision methods from a single-granularity perspective can render a significant amount of data ineffective, ultimately resulting in a loss of credibility in the decision outcome. Therefore, designing MG decision-making methods is an indispensable step in addressing the rebalancing problem for UDBSS. Qian (2010) extended traditional rough set theory to MG rough sets, achieving information fusion through selection methods, including optimistic MG rough sets and pessimistic MG rough sets. Furthermore, when dealing with large-scale problems, Qian introduced the concept of local MG decision-theoretic rough sets to address the significant computational time required for approximate calculations in MG rough sets and the limitations of supervised learning (Qian et al., 2014, 2017). Li et al. (2022) put forward a local multi-granulation rough set model applicable in ordered information systems and conducted comparative analyses with global MG probability rough sets. Zhang et al. (2020) introduced MG decision-theoretic rough sets in the context of hesitant fuzzy linguistic term sets, developing an MG GDM method based on this framework. Li and Xu (2015) introduced the double-quantitative decision-theoretic rough sets by improving the MG rough set. Subsequently, Xu and Guo (2016) further extended this concept to the generalized MG double-quantitative decision-theoretic rough sets. Zhang et al. (2021) proposed the adjustable MG PRSs model, extending it to the dual hesitant fuzzy environment, providing DM with a broader range of granularity choices.

TWD, as one of the decision-making paradigms, was introduced by Yao (2010), (2021) based on the rough set theory. It divides the universe of discourse into three parts, corresponding to the positive region (*POS*), negative region (*NEG*), and boundary region (*BND*) in rough sets, and assigns them strong interpretative semantics and classification methods. This idea helps people to give another cognitive attitude, that is, "no-commitment", when they are faced with complex problems and cannot make an attitude of "accept" or "reject". It changes the two classification methods into three classification methods, which is closer to the cognitive model of human beings (Yao, 2016). In recent years, the TWD method has been extended to various fields, including clustering (Yu et al., 2020), deep learning (Cheng et al., 2021), and sentiment analysis (Zhang and Min, 2016), among others. Therefore, applying the TWD method to MG decision-making problems is essential. In 2018, Yao (2018) combined the TWD approach with granular computing and proposed three-way granular thinking. Scholars have also developed various methods for region partition. Yao (2010), using PRSs as the basis, provided rules for partitioning different regions. Subsequently, Liu et al. (2011) improved the loss function in the above method and introduced the concept of relative loss functions. Furthermore, Jia and Liu (2019) made the computation of loss functions objective and proposed a TWD method based on evaluation values. This method makes the classification thresholds obtained based on loss functions more objective, significantly enhancing the credibility of classification results in the TWD method.

As an MG decision-making method, the adjustable MG PRSs model exhibits effective fusion of MG fuzzy information and is straightforward to operate, performing well when dealing with complex MG problems. Furthermore, in the context of the evaluation value-based TWD method, the classification rules align with the upper and lower approximation partitioning methods of PRSs. Additionally, when addressing complex problems, the three-classification pattern offers DMs a buffer zone, reducing the error rate in decision-making. Therefore, incorporating the evaluation value-based TWD method into the adjustable MG PRSs model is more advantageous for solving the rebalancing problem for UDBSS.

2.3. Introduction to the behavioral decision theory

In the decision-making process, DMs often struggle to achieve a state of complete rationality because psychological factors can influence the decision outcome, leading to decisions that are not necessarily optimal. Traditional utility theories based on perfect rationality fail to model this scenario effectively. To bridge this gap, Kahnema and Tversk (1979) introduced PT in 1979, introducing bounded rationality into decision-making. This theory posits that individuals compare options against a reference point when faced with different choices, exhibiting risk-averse behavior towards gains and risk-taking behavior towards losses. Subsequently, in 1982, Bell (1982), Loomes and Sugden (1982) refined PT with the introduction of RT. They argued that DMs, after making a choice, focus more on the gap between the current outcome and alternative choices rather than solely on the current outcome itself, emphasizing relative value over absolute value. These two theories respectively address the influence of psychological factors during and after the decision-making process, effectively incorporating DMs' bounded rationality into the outcomes.

In recent years, bounded rationality theories, including PT and RT, have found widespread application in the field of intelligent decision-making. Researchers like Wan et al. (2020) considered DMs' bounded rationality in heterogeneous multi-attribute GDM problems, integrating PT and using the ideal solution as a reference point to calculate gains and losses. Wang et al. (2020), (2022), on the foundation of TWD, incorporated both PT and RT. Zhang et al. (2023), in the context of incomplete T-spherical fuzzy information systems, constructed an MG TWD model based on RT.

In summary, the bounded rationality of DMs is an essential factor in the decision-making process. However, PT and RT analyze DMs' psychological states from two different perspectives. Therefore, we propose a combined approach that integrates both to characterize bounded rationality phenomena and incorporate them into the decision-making process. The inclusion of this approach in the rebalancing model for UDBSS can better reflect user behavioral logic and reduce decision-making errors.

2.4. Introduction to the rebalancing problem for UDBSS

Currently, research on the rebalancing problem for UDBSS can be primarily divided into two aspects: dynamic rebalancing and static rebalancing.

First, dynamic rebalancing addresses the allocation of bikes based on real-time data during the daytime when bike usage is high, with the goal of achieving rapid decision-making and action. Current research focuses on minimizing relocation costs or unmet demand. Brinkmann et al. (2019) proposed a dynamic lookahead policies that predicts potential demand in the current environment using dynamic programming, achieving minimization of unmet demand. You (2019) developed a constrained mathematical model using a periodic review relocation strategy, aiming to minimize the sum of unmet demand and transportation costs. Cai et al. (2022), taking into account damaged bikes, used an adaptive routing strategy to maximize the expected overall demand, including relocation and damaged bike recovery demand. They adjusted the transport team's routes according to actual demand, ensuring a vehicle balance at different stations with the smallest team size. On the other hand, static rebalancing involves predicting and allocating bikes for the next day based on historical data during the nighttime when bike usage is lower. Zhang (2022) introduced a "pickup or delivery" rule to optimize repositioning rules and plan action routes based on this approach to minimize total costs. Dell'Amico et al. (2016) designed a destroy and repair metaheuristic algorithm that reduces the computational effort needed for neighborhood exploration. They applied this algorithm to solve the bicycles allocation routing problem, achieving good results.

Much of the literature (Bulhões et al., 2018; Tian et al., 2020; Zhang et al., 2020) has focused on path optimization for the distribution of dockless bikes in terms of cost minimization. However, few articles have paid significant attention to resident demand. Therefore, this paper designs a static rebalancing model for UDBSS based on residents' daily usage preferences, including bike usage and return, with the goal of minimizing unmet resident demand.

3. Basic knowledge

In this section, CIFSs, PRSs and TWD methods are briefly reviewed to facilitate the subsequent experiments.

3.1. CIFs

In IFSs, data features are described by MD and ND. However, it has certain limitations, that is, its ability to express information is relatively weak. In order to improve its ability to express information, Alkouri and Salleh (Garg and Rani, 2019) extended the concept of IFS to the complex number field, and proposed CIFSs by combining them. At present, CIFSs have a good performance in expressing two-dimensional information in fuzzy environments.

Definition 3.1. Alkouri and Salleh (2012) Suppose a CIFS C, defined in a non-empty finite universe of discourse U, is given as:

$$C = \{(x, \mu_C(x), \rho_C(x)) | x \in U\}$$

where $\mu(x) = r_C(x)e^{2\pi j\omega_C(x)}$ and $\rho(x) = k_C(x)\ e^{2\pi j\varpi_C(x)}$ denote MD and ND of arbitrary $x \in U$ to the set C, respectively. For simplicity, this article will abbreviate the expression as $\mu = r_C e^{2\pi j\omega_C}$ and $\rho\ = k_C e^{2\pi j\varpi_C}$. Further, real part $r_C, k_C : U \to [0,1]$ represent amplitude value of μ and ρ, imaginary part $j = \sqrt{-1}$ and $\omega_C, \varpi_C : U \to [0,1]$ represent phase value of ones, meeting $0 \le r_C + k_C \le 1$ and $0 \le \omega_C + \varpi_C \le 1$. Based on the principle of convenience of expression, we structure this pair $\gamma\ = (r_\gamma, \omega_\gamma, k_\gamma, \varpi_\gamma)$and call it as a complex intuitionistic fuzzy number (CIFN).

For the sake of further describing more complicated information from the real world, the CIF relation is structured by extending CIFSs to the dual-universe environment.

Definition 3.2. Suppose U and V are two finite universes of discourse. A CIF relation R in terms of $U \times V$ is given by

$$R = \{\langle (x, y), \mu_R(x, y), \rho_R(x, y)\rangle | (x, y) \in U \times V\}.$$

In this paper, some basic algorithms of CIFSs are needed to solve decision-making problems in CIFSs environment.

Definition 3.3. Garg and Rani (2019) Let $\gamma_j\ = (r_j, \omega_j, k_j, \varpi_j), j = 1, 2$ be two arbitrary CIFNs, then, we can get

(1) $\gamma_1 \oplus \gamma_2 = ((r_1 + r_2 - r_1 r_2), (\omega_1 + \omega_2 - \omega_1\omega_2), k_1 k_2, \varpi_1\varpi_2),$
(2) $\gamma_1 \otimes \gamma_2 = (r_1 r_2, \omega_1\omega_2, (k_1 + k_2 - k_1 k_2), (\varpi_1 + \varpi_2 - \varpi_1\varpi_2)),$
(3) $\lambda\gamma_1\ = (1 - (1 - r_1)^\lambda, (1 - (1 - \omega_1)^\lambda), k_1^\lambda, \varpi_1^\lambda),$
(4) $\gamma_1^\lambda\ = (r_1^\lambda, \omega_1^\lambda, 1 - (1 - k_1)^\lambda, (1 - (1 - \varpi_1)^\lambda)),$
(5) the complement of γ_1: $\gamma_1^c\ = (k_1, \varpi_j, r_1, \omega_j).$

In order to facilitate the comparison of different CIFN, then obtain the final ordering results of multiple elements and find the maximum or minimum value, it is necessary to introduce the score function and the precision function of CIFNs.

Definition 3.4. Define a CIFN $\gamma\ = (r_\gamma,\ \omega_\gamma,\ k_\gamma,\ \varpi_\gamma)$, then the score function $Sc(\gamma)$ and the accuracy function $H(\gamma)$ of γ is given by

$$Sc(\gamma) = r_\gamma - k_\gamma + \omega_y - \varpi_\gamma, \tag{1}$$

$$H(\gamma) = r_\gamma + k_\gamma + \omega_\gamma + \varpi_\gamma, \tag{2}$$

where $Sc(\gamma) \in [-2, 2]$ and $H(\gamma) \in [0, 2]$. Moreover, suppose γ_1 and γ_2 are two CIFNs, the ordered relation between γ_1 and γ_2 can be obtained based on Formula (1) and (2):

(1) If $Sc(\gamma_1) > Sc(\gamma_2)$, then $\gamma_1 \succ \gamma_2$,
(2) If $Sc(\gamma_1) < Sc(\gamma_2)$, then $\gamma_1 \prec \gamma_2$,
(3) If $Sc(\gamma_1)\ = Sc(\gamma_2)$, then
  1) If $H(\gamma_1) > H(\gamma_2)$, then $\gamma_1 \succ \gamma_2$,
  2) If $H(\gamma_1) < H(\gamma_2)$, then $\gamma_1 \prec \gamma_2$,
  3) If $H(\gamma_1)\ = H(\gamma_2)$, then $\gamma_1 \sim \gamma_2$.

In this paper, in order to accurately describe the relationship between two CIFNs in the process of problem decision, it is necessary to use the method of measuring distance.

Definition 3.5. Rani and Garg (2017) Given two CIFNs $\gamma_j = (r_j, \omega_j,\ k_j,\ \varpi_j), j = 1, 2$, then the distance between γ_1 and γ_2 is got by the following formula:

$$d(\gamma_1, \gamma_2) = \frac{1}{4}(|r_1 - r_2| + |k_1 - k_2| + |\omega_1 - \omega_2| + |\varpi_1 - \varpi_2|) \tag{3}$$

similarly, it is clear that $d(\gamma_1, \gamma_2) \in [0, 1]$.

3.2. PRSs

When applying classical rough set theory to establish approximate spaces, strict rules often leave little room for adjustment when dealing with classification errors. In addressing this challenge, Yao (2010) introduced the notion of PRSs. These employ conditional probability and two thresholds to formulate rough approximations, providing a more flexible approach compared to the rigid construction rules of classical rough approximations.

Definition 3.6. Yao (2010) Suppose R is an equivalence relation in finite universe of discourse U, and P is a probability measure, then (U, R, P) is named as probabilistic approximation space. For arbitrarily $X \subseteq U$, the upper and lower approximations of X with respect to (U, R, P) are provided by:

$$\underline{R}^\alpha(X) = \{x \in U | P(X|[x]) \ge \alpha\}, \tag{4}$$

$$\overline{R}^\beta(X) = \{x \in U | P(X|[x]) > \beta\}, \tag{5}$$

where the parameters meet $0 \le \beta < \alpha \le 1$. Then, $\left(\underline{R}^\alpha(X), \overline{R}^\beta(X)\right)$ is titled a PRS. Then, it is naturally divided into three independent parts, which are defined as:

$$POS(X) = \underline{R}^\alpha(X), \tag{6}$$

$$BND(X) = \overline{R}^\beta(X) - \underline{R}^\alpha(X), \tag{7}$$

$$NEG(X) = U - \overline{R}^\beta(X). \tag{8}$$

3.3. Evaluation value-based TWD methods

Given the superiority of TWD in the field of MG decision-making, this paper applies the evaluation value-based TWD methods to the rebalancing problem for UDBSS. Below, the development process of the three decisions is introduced in detail.

In the classic MG decision-making process, the DM defines the alternative set with m elements and the attribute set with n elements respectively as $U = \{x_1, \cdots, x_j, \cdots, x_m\}$ and $V\ = \{y_1, \cdots, y_h, \cdots, y_n\}$. Then, all attributes of each alternative are evaluated by experts to generate an evaluation matrix $R\ = (e_{jh})_{m\times n}$, in which the value e_{jh} is the evaluation value of y_h with respect to x_j. And also, the weight set of n attributes is expressed as $\boldsymbol{u}\ =\ \{u_1, \cdots, u_h, \cdots, u_n\}^{\mathrm{T}}$, which satisfies $u_h \in [0, 1]$ $(1 \le h \le n)$ and $\sum_{h=1}^n u_h\ = 1$.

On the basis of probabilistic rough sets, Yao (2010) proposed a TWD model and give a reasonable semantic interpretation of these three regions and proposed the loss functions of different decision results in two states. Supposing there are three decision results in the action set $A\ = \{a_P, a_B, a_N\}$, which separately represent $x \in POS$,$x \in BND$, $x \in NEG$, correspond to acceptance, non-commitment and rejection. Then, the state set $\Omega = \{V, \neg V\}$ show that an alternative is in V or not in V. In view of these two dimensions, we can achieve the loss function matrix with respect to the cost of three actions in two states, which is presented as Table 1 below.

In this table, $\lambda_{PP}, \lambda_{BP}, \lambda_{NP}$ denote the cost that an alternative x_j is classified into region POS, BND, NEG when $x_j \in V$, similarly, $\lambda_{PN}, \lambda_{BN}$, λ_{NN} denote the cost that one is classified into region POS, BND, NEG when $x_j \notin V$. Further, if we assume $\lambda_{PP}\ = 0$ and $\lambda_{NN}\ = 0$, it means there

Table 1
Loss function.

	$V(POS)$	$\neg V(NEG)$
a_P	λ_{PP}	λ_{PN}
a_B	λ_{BP}	λ_{BN}
a_N	λ_{NP}	λ_{NN}

is no loss when classification is correct. Accordingly, other costs are also needed to be reduced, namely, $\lambda^{'}_{BP} = \lambda_{BP} - \lambda_{PP}$, $\lambda^{'}_{NP} = \lambda_{NP} - \lambda_{PP}$, $\lambda^{'}_{PN} = \lambda_{PN} - \lambda_{NN}$ and $\lambda^{'}_{BN} = \lambda_{BN} - \lambda_{NN}$. Then the loss function in Table 1 can be converted into a relative loss function, as shown in Table 2 (Liu et al., 2011).

Considering relative loss function still owns subjectivity, Jia and Liu (2019) put forward evaluation value-based TWD method by introducing evaluation value e_{jh} and the parameter σ, where $\sigma \in [0, 0.5]$ and denotes the preference of DM on risk. Then we can obtain the relative loss function based on evaluation values, which is described as Table 3.

By virtue of Table 3, the formulas of two threshold α_{jh} and β_{jh} are given below.

$$\alpha_{jh} = \frac{(1-\sigma)(1-e_{jh})}{(1-\sigma)(1-e_{jh}) + \sigma e_{jh}}, \tag{9}$$

$$\beta_{jh} = \frac{\sigma(1-e_{jh})}{\sigma(1-e_{jh}) + (1-\sigma)e_{jh}}. \tag{10}$$

Remark 3.1. This model adeptly mitigates subjectivity-induced losses when the DMs takes varying actions in different states. This enhances the objectivity of decision outcomes. Additionally, the model offers an innovative approach to establish personalized threshold values. It achieves this by autonomously computing thresholds for each alternative based on their respective attribute evaluation values, thereby minimizing the likelihood of classification errors. The TWD methods used in the subsequent model introduction all refer to evaluation value-based TWD methods.

4. Adjustable MG CIF PRS based on P-RT

Within this section, we present a novel data processing approach known as adjustable MG CIF PRSs. This method is introduced to tackle the challenges posed by MG decision-making problems, specifically targeting the complexities of choosing the most appropriate granularity and establishing thresholds objectively. Subsequently, we delve into the P-RT, a concept aimed at emulating the psychological states of DMs. The primary objective of this technique is to enhance the alignment of decision outcomes with real-world scenarios, thereby improving the overall accuracy and practicality of the decision-making process. To further capture the often irrational nature of DMs during the decision-making process, we seamlessly integrate the P-RT into the construction of PRSs. This pioneering approach, referred to as Adjustable MG CIF PRSs based on P-RT, serves as a robust methodological underpinning for subsequent rebalancing models for UDBSS, offering valuable insights into enhancing decision-making practices.

In MG GDM problems, suppose $U = \{x_1, \cdots, x_j, \cdots, x_m\}$ and $V = \{y_1, \cdots, y_h, \cdots, y_n\}$ are the alternative set. The DM set is recorded as $Z = \{z_1, \cdots, z_i, \cdots, z_l\}$, and its corresponding weight set is $\boldsymbol{w} = \{w_1, \cdots, w_i, \cdots, w_l\}^{\mathrm{T}}$. The assess matrices is defined as $R_i = (e^i_{jh})_{m\times n} (i = 1, 2, \cdots, l)$ and $S = \{s_1, \cdots, s_h, \cdots, s_n\}$ is a standard assessment set. Symbol e^i_{jh} represent an evaluation value of j-th alternative by i-th DM under h-th attribute. Lastly, $\boldsymbol{u_i} = \{u_{i1}, \cdots, u_{ih}, \cdots, u_{in}\}^{\mathrm{T}}$ is the weight set of relation set R_i corresponding to set V.

Table 2
Relative loss functions.

	$V(POS)$	$\neg V(NEG)$
a_P	0	$\lambda^{'}_{PN}$
a_B	$\lambda^{'}_{BP}$	$\lambda^{'}_{BN}$
a_N	$\lambda^{'}_{NP}$	0

Table 3
Relative loss functions based on evaluation values.

	$V(POS)$	$\neg V(NEG)$
a_P	0	$1 - e_{jh}$
a_B	σe_{jh}	$\sigma(1 - e_{jh})$
a_N	e_{jh}	0

4.1. The adjustable MG CIF PRSs based on TWD methods

In this section, we have produced a new and iconic MG CIF PRSs model by integrating prs into the MG CIF environment. This model, coherently combined with the principles outlined in Section 4.2, culminates in a model capable of categorizing all available alternatives into three distinct regions. Furthermore, through this integration and refinement process, we effectively derive sorted results that illuminate the decision landscape with greater clarity and precision.

Definition 4.1. Let (U, V, R_i, S) be an MG CIF information system. Then, the single CIF evaluation value of x_j of R_i can be achieved by the formula below,

$$\theta^{R_i}_S(x_j) = \frac{\sum_{h=1}^{n} u_h e^i_{jh} s_h}{\sum_{h=1}^{n} u_h e^i_{jh}}. \tag{11}$$

In this formula, the division operator for CIFN is used. Therefore, we provide a suitable division operator, which is shown as formula

$$\begin{aligned} \gamma_1 \odot \gamma_2 = & \left(\min\left(1, \frac{r_1}{r_2}\right) e^{2\pi j \min\left(1, \frac{\omega_1}{\omega_2}\right)}, \right. \\ & \left. \max\left(0, \frac{k_1 - k_2}{1 - k_2}\right) e^{2\pi j \max\left(0, \frac{\varpi_1 - \varpi_2}{1 - \varpi_2}\right)} \right), \end{aligned} \tag{12}$$

where $\gamma_j = (r_j, \omega_j, k_j, \varpi_j), j = 1, 2$ are two arbitrary CIFNs.

In order to select a final evaluation value of x_j from all $\theta^{R_i}_S(x_j)$reasonably, the single CIF evaluation value of x_j on all DMs need to be ordered.

Definition 4.2. Suppose $\theta^{R_{\tau(i)}}_S(x_j)$ is an adjustable single CIF evaluation value of x_j, generated by arranged $\theta^{R_i}_S(x_j)$ of x_j in an ascending order. $\eta = i/l (i = 1, 2, \cdots, l)$ Express the DM's preference for risk, meaning selecting the i-th smallest value among all evaluation values of x_j as final assess value and the larger the value of i, the more likely the DM is to pursue risk.

The single CIF MD of x_j on R_i are obtained through Definition 4.1 Then, after determining the adjustable single CIF MD parameter τ, we can obtain final assessing value of x_j. The more we prefer risk, the larger parameter τ, the greater the selected final MD $\theta^{R_{\tau(i)}}_S(x_j)$ of x_j. Next, the threshold value α^i_j and β^i_j can be got by replacing e_{jh} in the Formula (9) and (10) with $\theta^{R_i}_S(x_j)$, which are used to determine the final thresholds in next section.

Remark 4.1. In contrast to the earlier proposals of optimistic and pessimistic rough sets, which were limited to selecting either the minimum or maximum granularity, the adjustable variant of rough sets introduced in this section presents a substantial advancement. It efficiently addresses the issue of excessively extreme granularity selection. Within this adjustable rough set framework, the sorting of membership degrees not only facilitates the determination of both minimum and maximum granularity levels but also affords the ability to select a more balanced and moderate granularity. This enhanced flexibility empowers decision-makers to navigate a broader spectrum of granularity options, optimizing their choices for more nuanced and well-informed decision-making processes. For example, when $\eta = 3/4$, meaning the third of all sorted membership degrees of $x_j (j = 1, 2, \cdots m)$ is selected.

4.2. P-RT

Prior to the introduction of the concept of bounded rationality, there was a prevailing belief that DMs operated under complete rationality during the decision-making process. This perspective largely disregarded the influence of psychological factors on decision outcomes. However, in the following sections, we integrate the P-RT into our model. This integration is executed through a systematic four-step process, leveraging P-RT as a method for selecting classification thresholds. By doing so, we achieve a more effective simulation of bounded rationality, accounting for the inherent complexities of human decision-making influenced by psychological factors.

(1) Calculate positive and negative ideal threshold of each alternative x_j, where $j = 1, 2, \cdots, m$, denoted as:

$$P_\alpha = \left\{p_j^\alpha\right\} = \left\{\max_{i=1,2,\cdots,l}(\alpha_{1i}), \max_{i=1,2,\cdots,l}(\alpha_{2i}), \cdots, \max_{i=1,2,\cdots,l}(\alpha_{mi})\right\}, \tag{13}$$

$$N_\alpha = \left\{n_j^\alpha\right\} = \left\{\min_{i=1,2,\cdots,l}(\alpha_{1i}), \min_{i=1,2,\cdots,l}(\alpha_{2i}), \cdots, \min_{i=1,2,\cdots,l}(\alpha_{mi})\right\}, \tag{14}$$

$$P_\beta = \left\{p_j^\beta\right\} = \left\{\max_{i=1,2,\cdots,l}(\beta_{1i}), \max_{i=1,2,\cdots,l}(\beta_{2i}), \cdots, \max_{i=1,2,\cdots,l}(\beta_{mi})\right\}, \tag{15}$$

$$N_\beta = \left\{n_j^\beta\right\} = \left\{\min_{i=1,2,\cdots,l}(\beta_{1i}), \min_{i=1,2,\cdots,l}(\beta_{2i}), \cdots, \min_{i=1,2,\cdots,l}(\beta_{mi})\right\}. \tag{16}$$

(2) Calculate positive and negative values of thresholds of x_j according to the formulas

$$v_{ji}^{\alpha+} = \left(\Delta Sc_{ji}^{\alpha+}\right)^\xi = \left(Sc(\alpha_{ji}) - Sc\left(n_j^\alpha\right)\right)^\xi, \tag{17}$$

$$v_{ji}^{\alpha-} = -\kappa\left(-\Delta Sc_{ji}^{\alpha-}\right)^\zeta = -\kappa\left(Sc\left(p_j^\alpha\right) - Sc(\alpha_{ji})\right)^\zeta, \tag{18}$$

$$v_{ji}^{\beta+} = \left(\Delta Sc_{ji}^{\beta+}\right)^\xi = \left(Sc(\beta_{ji}) - Sc\left(n_j^\beta\right)\right)^\xi, \tag{19}$$

$$v_{ji}^{\beta-} = -\kappa\left(-\Delta Sc_{ji}^{\beta-}\right)^\zeta = -\kappa\left(Sc\left(p_j^\beta\right) - Sc(\beta_{ji})\right)^\zeta, \tag{20}$$

where these four values express the values of losses and benefits. It should be noted that the parameters ξ and ζ convey the degree of sensitivity of the DMs to loss and benefit, both of which are between zero and one.

(3) Calculate positive and negative prospect values and total prospect values for each DM, which are determined by

$$V_i^{\alpha+} = \sum_{j=1}^m v_{ji}^{\alpha+} w_j^+, V_i^{\alpha-} = \sum_{j=1}^m v_{ji}^{\alpha-} w_j^-, \tag{21}$$

$$V_i^\alpha = V_i^{\alpha+} + V_i^{\alpha-}, \tag{22}$$

$$V_i^{\beta-} = \sum_{j=1}^m v_{ji}^{\beta-} w_j^-, V_i^{\beta-} = \sum_{j=1}^m v_{ji}^{\beta-} w_j^-, \tag{23}$$

$$V_i^\beta = V_i^{\beta+} + V_i^{\beta-}, \tag{24}$$

where positive and negative weight of x_j are recorded as $w_j^+ = \frac{w_j^\phi}{\left(w_j^\phi + (1-w_j)^\phi\right)^{1/\phi}}$ and $w_j^- = \frac{w_j^\varphi}{\left(w_j^\varphi + (1-w_j)^\varphi\right)^{1/\varphi}}$. These parameters $\phi \in (0, 1)$ and $\varphi \in (0, 1)$ reflect different attitudes when DM face on gain and loss.

(4) Calculate prospect-regret (P-R) value of each DM on two thresholds by means of

$$PRV^\alpha(R_i) = V_i^\alpha + \sum_{o=1}^m \left(1 - e^{-\delta_i\left(V_i^\alpha - V_o^\alpha\right)}\right), \tag{25}$$

$$PRV^\beta(R_i) = V_i^\beta + \sum_{o=1}^m \left(1 - e^{-\delta_i\left(V_i^\beta - V_o^\beta\right)}\right), \tag{26}$$

where parameter $\delta_i (\delta_i \geq 0)$ mean the different regret avoidance abilities of each DM. This function reflects regret-rejoice values of DMs, and it is an increasing concave function monotonically, which describes that DMs are more sensitive to regret than to rejoice. Further, the greater the δ, the stronger the ability to avoid regret.

(5) Determine final thresholds

After determining distinct P-R values for all DMs with respect to the two thresholds, our next step involves the selection of the final threshold. This critical decision is guided by the threshold recommended by the decision-maker with the highest P-R value, which are expressed as $\alpha_{j,final}$ and $\beta_{j,final}$.

On the basis of Section 4.1, we use P-RT to obtain the final thresholds in the state of bounded rationality. They will be applied in our model.

5. The rebalancing model for UDBSS based on MG PRS and P-RT in CIF information system

In this section, we introduce a rebalancing model for UDBSS that leverages the MG GDM approach. We offer a detailed exposition of the model's practical application and its intricate algorithmic framework. Through the utilization of this model, we are equipped to make precise forecasts regarding UDBSS demand at multiple locations, thereby facilitating a more judicious allocation of UDBSS resources. This model represents a valuable tool for optimizing the distribution of resources to meet demand effectively and efficiently across diverse locations.

5.1. The application of rebalancing models for UDBSS

Prior to applying the data, it is essential to preprocess the required data using suitable methods. To employ the rebalancing model for UDBSS presented in this article, it is imperative to convert all data into the CIFN format. Subsequently, we outline the rebalancing model for UDBSS as follows.

First, we need to construct MG CIF information system (U, V, R_i, S), as described in Section 4.1. Specifically, the evaluation value e_{jh}^i and standard assessment number s_h are both CIFNs. It is showed as Table 4. Then, calculate the weights of alternatives and DMs using the maximum deviation method. The specific formula is as follows.

$$u_{ih} = \frac{\sum_{j=1}^m \sum_{o=1}^m \left(d\left(e_{jh}^i, e_{oh}^i\right)\right)}{\sum_{h=1}^n \sum_{j=1}^m \sum_{o=1}^m \left(d\left(e_{jh}^i, e_{oh}^i\right)\right)}, \tag{27}$$

Table 4
The MG CIF information system.

	R_1				R_2				$\cdots$	R_l			
	y_1	y_2	$\cdots$	y_n	y_1	y_2	$\cdots$	y_n	$\cdots$	y_1	y_2	$\cdots$	y_n
x_1	e^1_{11}	e^1_{12}	$\cdots$	e^1_{1n}	e^2_{11}	e^2_{12}	$\cdots$	e^2_{1n}	$\vdots$	e^l_{11}	e^l_{12}	$\cdots$	e^l_{1n}
x_2	e^1_{21}	e^1_{22}	$\cdots$	e^1_{2n}	e^2_{21}	e^2_{22}	$\cdots$	e^2_{2n}	$\vdots$	e^l_{21}	e^l_{22}	$\cdots$	e^l_{2n}
$\vdots$	$\vdots$	$\vdots$	$\ddots$	$\vdots$	$\vdots$	$\vdots$	$\ddots$	$\vdots$	$\vdots$	$\vdots$	$\vdots$	$\ddots$	$\vdots$
x_m	e^1_{m1}	e^1_{m2}	$\cdots$	e^1_{mn}	e^2_{m1}	e^2_{m2}	$\cdots$	e^2_{mn}	$\vdots$	e^l_{m1}	e^l_{m2}	$\cdots$	e^l_{mn}

$$w_i = \frac{\sum_{h=1}^{n}\sum_{o=1}^{n}(|u_{ih} - u_{io}|)}{\sum_{i=1}^{l}\sum_{h=1}^{n}\sum_{o=1}^{n}(|u_{ih} - u_{io}|)}. \tag{28}$$

Remark 5.1. This approach involves quantifying disparities among all objects and posits that objects with more substantial distinctions from their counterparts exert a more significant influence on the decision-making process. Consequently, such objects merit a higher weight or priority in the decision-making process.

Next, in order to classify these alternatives and get optimal one by ranking them, we need to perform data fusion operations. Via Formula (11), the single evaluation value $\theta_S^{R_i}(x_j)$ of x_j of R_i is gotten and standard assessment set is reflected as

$$S(y_h) = \{\langle y_1, (r_1, \omega_1, k_1, \varpi_1)\rangle, \cdots, \langle y_h, (r_h, \omega_h, k_h, \varpi_h)\rangle,$$

$$\cdots\langle y_n, (r_n, \omega_n, k_n, \varpi_n)\rangle\}.$$

In this formula,

$$r_h = \frac{\sum_{i=1}^{l}\sum_{j=1}^{m} r_{ijh}}{l * m}, \omega_h = \frac{\sum_{i=1}^{l}\sum_{j=1}^{m} \omega_{ijh}}{l * m}, \tag{29}$$

$$k_h = \frac{\sum_{i=1}^{l}\sum_{j=1}^{m} k_{ijh}}{l * m}, \varpi_h = \frac{\sum_{i=1}^{l}\sum_{j=1}^{m} \varpi_{ijh}}{l * m}. \tag{30}$$

At this point, the evaluation matrix transforms into $R = (\theta_S^{R_i}(x_j))_{m\times l}$, $i = 1, 2, \cdots, l$, which is given as Table 5.

Further, the classification and sorting tasks are completed by utilizing it. For classification tasks, ranking in ascending order is primary, and our preference for risk determines the selection result of final assessing value of x_j. On this basis, the final assessing value $\theta_S^{R_{\tau(i)}}(x_j)$ of $x_j$is gotten according to Definition 4.2. On the other hand, the thresholds α_j^i and β_j^i of x_j can be obtained by replacing e_{jh} in Formula (9) and (10) with $\theta_S^{R_i}(x_j)$ and are shown as:

$$\alpha_j^i = \frac{(1-\vartheta)\left(1-\theta_S^{R_i}(x_j)\right)}{(1-\vartheta)\left(1-\theta_S^{R_i}(x_j)\right) + \vartheta\theta_S^{R_i}(x_j)}, \tag{31}$$

$$\beta_j^i = \frac{\vartheta\left(1-\theta_S^{R_i}(x_j)\right)}{\vartheta\left(1-\theta_S^{R_i}(x_j)\right) + (1-\vartheta)\theta_S^{R_i}(x_j)}, \tag{32}$$

which are used to divide upper and lower approximations. And the integrated parameter $\vartheta = \sum_{i=1}^{l} w_i\sigma_i$, which can integrate the risk preferences of all DMs and pay more attention to the role of individual opinions in the decision-making process.

Table 5
The single MG CIF information system.

	R_1	R_2	$\cdots$	R_l
x_1	$\theta_S^{R_1}(x_1)$	$\theta_S^{R_2}(x_1)$	$\cdots$	$\theta_S^{R_l}(x_1)$
x_2	$\theta_S^{R_1}(x_2)$	$\theta_S^{R_2}(x_2)$	$\cdots$	$\theta_S^{R_l}(x_2)$
$\vdots$	$\vdots$	$\vdots$	$\ddots$	$\vdots$
x_m	$\theta_S^{R_1}(x_m)$	$\theta_S^{R_2}(x_m)$	$\cdots$	$\theta_S^{R_l}(x_m)$

Given the existence of multiple threshold pairs, it becomes imperative to employ the P-RT method introduced in Section 4.2 for selecting the ultimate threshold. Subsequently, we obtain $\alpha_{j,final}$ and $\beta_{j,final}$ of each x_j. Following this, in accordance with Definition 3.6, we compare the final assessment value obtained in Section 4.1 to the concluding threshold acquired in Section 4.2, resulting in the adjustable MG CIF PRSs $\left(\underline{\sum_{i=1}^{l} R_i}^{\tau,\alpha_{j,final}}(S), \overline{\sum_{i=1}^{l} R_i}^{\tau,\beta_{j,final}}(S)\right)$ of universe U, computed using Formulas (4) and (5), where

$$\underline{\sum_{i=1}^{l} R_i}^{\tau,\alpha_{j,final}}(S) = \left\{x \in U | \theta_S^{R_{\tau(i)}}(x_j) \geq \alpha_{j,final}\right\}, \tag{33}$$

$$\overline{\sum_{i=1}^{l} R_i}^{\tau,\beta_{j,final}}(S) = \left\{x \in U | \theta_S^{R_{\tau(i)}}(x_j) > \beta_{j,final}\right\}. \tag{34}$$

Thus, these following three classification rules are further determined in terms of Formulas (6) - (8).

$$POS^{\tau,\alpha_{j,final}}(X) = \underline{\sum_{i=1}^{l} R_i}^{\tau,\alpha_{j,final}}(S), \tag{35}$$

$$BND^{\tau,\alpha_{j,final},\beta_{j,final}}(X) = \overline{\sum_{i=1}^{l} R_i}^{\tau,\beta_{j,final}}(S) - \underline{\sum_{i=1}^{l} R_i}^{\tau,\alpha_{j,final}}(S), \tag{36}$$

$$NEG^{\tau,\beta_{j,final}}(X) = U - \overline{\sum_{i=1}^{l} R_i}^{\tau,\beta_{j,final}}(S). \tag{37}$$

Based on this, we can classify all alternatives into three discrete regions $POS^{\tau,\alpha_{j,final}}$, $BND^{\tau,\alpha_{j,final},\beta_{j,final}}$ and $NEG^{\tau,\beta_{j,final}}$, which represent acceptance, non- commitment and rejection, respectively.

Lastly, sort the final evaluation values $\theta_S^{R_{\tau(i)}}(x_j)$ of all alternatives using Definition 3.4, and adjust the sorting results under the constraint of criterion $POS^{\tau,\alpha_{j,final}} \succ BND^{\tau,\alpha_{j,final},\beta_{j,final}} \succ NEG^{\tau,\beta_{j,final}}$ to obtain the optimal alternatives.

5.2. The algorithm of rebalancing models for UDBSS

To offer a more concise and clear exposition of the model delineated in Section 5.1, we shall consolidate and outline the model's procedural steps within this section. This summarization serves the purpose of enhancing clarity and accessibility, facilitating a more comprehensive understanding of the model's operational framework.

Input: An MG CIF information system (U, V, R_i, S) after data preprocessing.

Output: Classification and sorting results for all alternatives.

Step 1: Calculate attribute weights u_{ih} and DM weights w_i according to Formula (27) and (28).

Step 2: Calculate adjustable single MG CIF information system based on Section 4.1 and determine the final evaluation.

Step 3: Calculate thresholds α_j^i and β_j^i based on Formulas (31) and (32).

Step 4: Select the final thresholds in terms of P-RT proposed in Section 4.2.

Step 5: Divide into three classification areas $POS^{\tau,\alpha_{j,final}}(X)$, $BND^{\tau,\alpha_{j,final},\beta_{j,final}}(X)$ and $NEG^{\tau,\beta_{j,final}}(X)$ with the help of Formulas (33) - (37).

Step 6: Determine the sorting result under the constraints of classification result.

Remark 5.2. Building upon the explanation provided earlier, we systematically compute the time complexities of the model introduced in this article. This process yields complexities for $O(ln^2)$, $O(lmn)$, $O(lm)$, $O(lm)$, $O(m)$ and $O(m)$, respectively. In summary, we can deduce that when n surpasses m, the overall time complexity of the model in this article is $O(ln^2)$. Similarly, when m exceeds n, it becomes $O(lmn)$.

By meticulously following the six outlined steps, we undertake a comprehensive refinement of the model, culminating in the formulation of its algorithm, which is detailed as Algorithm 1. This systematic process enhances the model's precision and effectiveness, laying the groundwork for its practical implementation and subsequent analysis.

Algorithm 1
The rebalancing model algorithm for UDBSS.

```
Input: MG CIF information system
Output: Classification and sorting results for all alternatives
Give the value of the parameter l, m, n, η, σ, δ.
  for i = 1 to l do
    for h = 1 to n do
      Calculate u_ih.
    end
      Calculate w_i.
end
for j = 1 to m do
  for i = 1 to l do
      Calculate θ_S^{R_i}(x_j).
  end
  Structure θ_S^{R_τ(i)}(x_j).
  Determine final assessing value.
  Calculate α_j^i and β_j^i.
end
for j = 1 to m do
    for i = 1 to l do
      Calculate PRV^α(R_i) and PRV^β(R_i).
      Determine α_{j,final} and β_{j,final}.
  end
end
for j = 1 to m do
    Categorize all the alternatives.
end
Sort based on classification results.
return Classification and sorting results.
```

6. Illustrative case studies

In this section, we aim to showcase the real-world applicability of the rebalancing model for UDBSS. We will begin with a specific UDBSS case and provide an in-depth investigation of the decision-making process using our model. The data set utilized for this demonstration is sourced from the Citi Bike System Data (https://citibikenyc.com/system-data). Moreover, we conducted sensitivity and comparative analyses based on the final experimental outcomes. These analyses serve to validate both the effectiveness and stability of our model.

6.1. The example description

In this case, under different weather conditions, according to the previous using and parking number of UDBSS in different locations, we conducted experimental analysis to judge the different demand for shared bicycles in these locations. Concretely, domains $U = \{x_1, x_2, x_3, x_4\}$ and $V = \{y_1, y_2, \cdots, y_{10}\}$ are the alternative set (the location codes are H101, H102, H103, H105) and attribute set (the date is from January 1st to January 10th) respectively, indicating the locations where the delivery number of bikes needs to be predicted. And all attributes include the number of bikes used a and the number of bikes parked b and weather in 15 days.

For the convenience of data processing, we have chosen specific data sets for statistical analysis, effectively converting them into a decision matrix. Our initial step involves the selection of four distinct locations as potential solutions. We then aggregate bicycle usage and returns at these locations from January 1st to January 10th, resulting in ten attributes. Additionally, we factor in weather conditions as uncertain variables for these 15 days. Recognizing that bicycle usage patterns vary during different time intervals, to introduce diversity into our data, we aim to avoid aggregating data across the entire day. Hence, we have divided the 24-hour statistical data into four segments: from 5 AM to 11 AM, from 11 AM to 3 PM, from 3 PM to 11 PM, and from 11 PM to 5 AM. These segments are treated as four distinct DMs and their details are recorded as follows: $Z = \{z_1, z_2, z_3, z_4\}$. For four DMs, four sets of binary relations $R_i = (e_{jh}^i)_{m\times n} \to U \times V (i = 1,2,3,4)$are given. The specific form is shown in Table 4.

After obtaining the decision matrix, the next step is to standardize the data and transform it into the CIFN format. This conversion process can be delineated into three distinct steps:

(1) Real part r of MD: This represents the using number of bicycles, and the larger the usage, the greater the demand. Consequently, for the parameter r, it is recommended to apply a benefit normalization formula, specifically Formula (38).

$$r_{jh} = \frac{a_{jh} - \min_j a_{jh}}{\max_j a_{jh} - \min_j a_{jh}}, \tag{38}$$

where $j = 1,2,3,4$ and $h = 1,2,\cdots,10$.

(1) Imaginary part ω of MD: This represents the parking number of bicycles. The larger the parking volume, the smaller the demand. Therefore, a cost normalization Formula (39) is used for parameter ω.

$$\omega_{jh} = \frac{\max_j b_{jh} - b_{jh}}{\max_j b_{jh} - \min_j b_{jh}}, \tag{39}$$

(2) Real part k and imaginary part ϖ of ND: In general, ND is a complement of MD, that is $k = 1 - r$ and $\varpi = 1 - \omega$. Nonetheless, uncertainty arises between MD and ND when we introduce uncertain factors. In this experiment, the uncertain factor under consideration is weather-related. Specifically, when weather conditions are either sunny or rainy, this uncertainty is manifested in real part k, denoted as $k = 0.75 \times (1 - r)$, resulting in an overall uncertainty of $1 - r - k$.

Once all the data has been successfully converted into CIFN format, we proceed to build the MG CIF information system, as illustrated in Table 4. Utilizing this system, we can then apply the model outlined in Section 5 for subsequent experimental analysis. The detailed decision-making process will be expounded upon in the following section.

Remark 6.1. Sunny or rainy weather conditions lead to a decrease in bicycle usage due to environmental factors, introducing uncertainty into the prediction of demand for a given location using current data. By employing Formula $k = 0.75 \times (1 - r)$, we express this uncertainty, signifying that as the number of bicycles used increases, the accuracy of predicting the highest demand for bicycles at the current location also increases, resulting in lower uncertainty. Conversely, higher uncertainty is associated with lower bicycle usage.

6.2. Detailed decision-making procedures

In this section, we embark on the practical implementation of the rebalancing model for UDBSS, as previously introduced in Section 5. Leveraging the foundation laid in Section 6.1 with the development of the MG CIF information system, we proceed to delve into an intricate exploration of the decision-making process associated with this model. This in-depth examination aims to provide a comprehensive and lucid understanding of how the model operates within the context of real-world rebalancing scenarios for UDBSS.

(1) Calculate weights of ten dates $u_{ih}(i = 1, 2, 3, 4; h = 1, 2, \cdots, 10)$ and weights of four time period $w_i(i = 1, 2, 3, 4)$ according to Formula (27) and (28). Therefore, we can get a concrete calculation, shown as Figs. 2 and 3.

(2) Calculate the standard assessment number $s_1 = (r_1, \omega_1, k_1, \varpi_1)$ and $r_1 = \frac{\sum_{i=1}^{l}\sum_{j=1}^{m} r_{ij1}}{4*4} = 0.54905$, $\omega_1 = \frac{\sum_{i=1}^{l}\sum_{j=1}^{m} \omega_{ij1}}{4*4} = 0.56039$. In a similar manner, we can easily obtain the following results.

$$s_1 = (0.54905 \quad 0.56039 \quad 0.45095 \quad 0.43961)$$
$$s_2 = (0.52146 \quad 0.53415 \quad 0.47854 \quad 0.46585)$$
$$s_3 = (0.45867 \quad 0.48403 \quad 0.46725 \quad 0.51597)$$
$$\vdots$$
$$s_{10} = (0.50403 \quad 0.54761 \quad 0.49597 \quad 0.45239)$$

Based on this, calculate single evaluation value of $x_j$in R_i by Formula (11). Then, sorting the single evaluation value in ascending order on the basis of the score function, the adjustable single MG CIF information system can be constructed, which is given in Table 6.

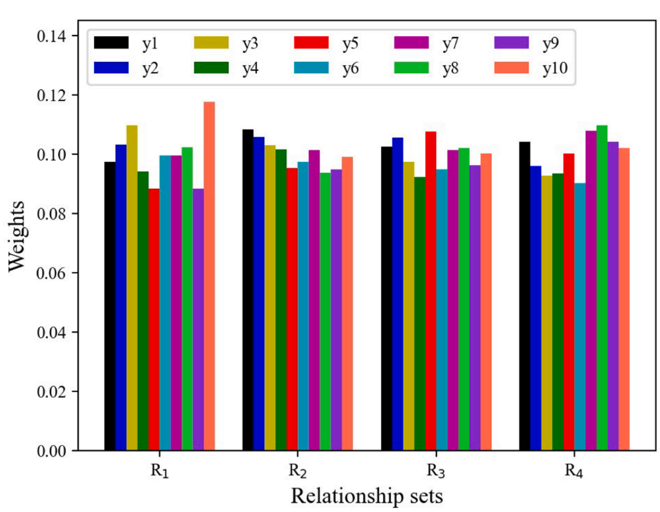

Fig. 2. Weights of ten dates in UDBSS instance.

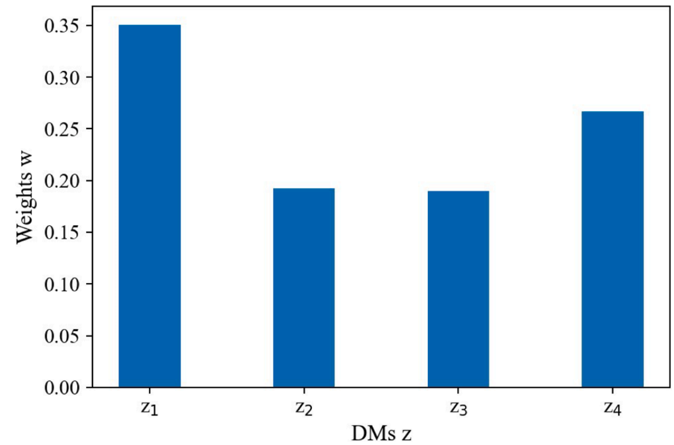

Fig. 3. Weights of four time period in UDBSS instance.

Table 6
The adjustable single MG CIF information system in the UDBSS instance.

	R_1	R_2	R_3	R_4
x_1	(0.54589, 0.68539, 0.39218, 0.31461)	(0.61724, 0.64636, 0.3359, 0.35364)	(0.57042, 0.69233, 0.37923, 0.30767)	(0.58090, 0.70900, 0.36437, 0.29098)
x_2	(0.63994, 0.53927, 0.29202, 0.46073)	(0.54903, 0.70115, 0.39446, 0.29885)	(0.68826, 0.61841, 0.2609, 0.38159)	(0.68909, 0.61701, 0.25839, 0.38299)
x_3	(0.57969, 0.61255, 0.36624, 0.38745)	(0.60461, 0.6439, 0.35957, 0.3561)	(0.69724, 0.62507, 0.25264, 0.37493)	(0.66503, 0.70675, 0.2853, 0.29325)
x_4	(0.55666, 0.64014, 0.38798, 0.35986)	(0.51732, 0.68784, 0.41789, 0.31216)	(0.60953, 0.6774, 0.33721, 0.3226)	(0.54614, 0.75779, 0.41697, 0.24221)

Subsequently, within the context of this experiment, we adopt a risk-neutral stance by assigning a risk preference parameter of $\eta = 3/4$. As a result, the ultimate evaluation values for all locations are determined by selecting the evaluation values provided within the relation set R_3. These chosen evaluation values are presented in the following manner:

$$\theta_S^{R_{r(3)}}(x_1) = (0.57042, 0.69233, 0.37923, 0.30767)$$
$$\theta_S^{R_{r(3)}}(x_2) = (0.68826, 0.61841, 0.2609, 0.38159)$$
$$\theta_S^{R_{r(3)}}(x_3) = (0.69724, 0.62507, 0.25264, 0.37493)$$
$$\theta_S^{R_{r(3)}}(x_3) = (0.60953, 0.6774, 0.33721, 0.3226)$$

(3) In the computational process, we proceed to calculate the thresholds α_j^i and β_j^i $(i, j = 1, 2, 3, 4)$ utilizing Formulas (31) and (32), with the parameter $\sigma = [0.25, 0.25, 0.25, 0.25]$. This particular choice signifies the unanimous adoption of a risk-neutral disposition by all DMs involved in the experiment. Furthermore, we introduce another parameter, denoted as ϑ, with a value of 0.25, as a parameter that integrates the attitudes of all DMs.

(4) In accordance with the P-RT introduced in Section 4.2, we proceed to compute the P-R values for each DM based on two thresholds, utilizing Formula (13) - (26). Notably, for this calculation, we assume uniform distribution of positive and negative weights for x_j, denoted as $w^+ = [0.25, 0.25, 0.25, 0.25]$ and $w^- = [0.25, 0.25, 0.25, 0.25]$. Ultimately, we arrive at the P-R values for all DMs concerning the two thresholds, as illustrated in Fig. 4.

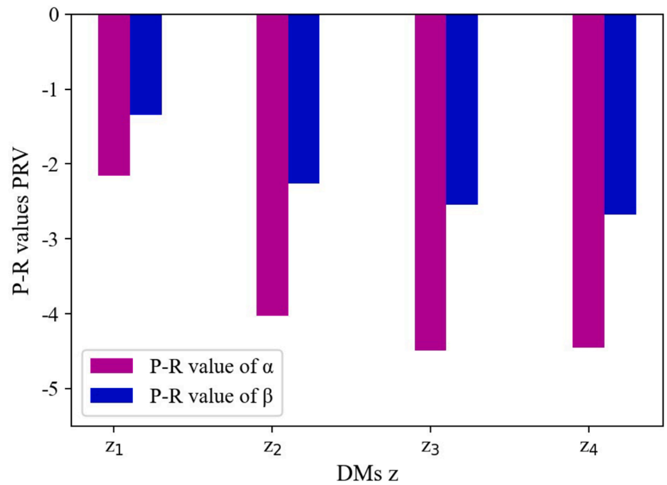

Fig. 4. the P-R values of DMs on two thresholds.

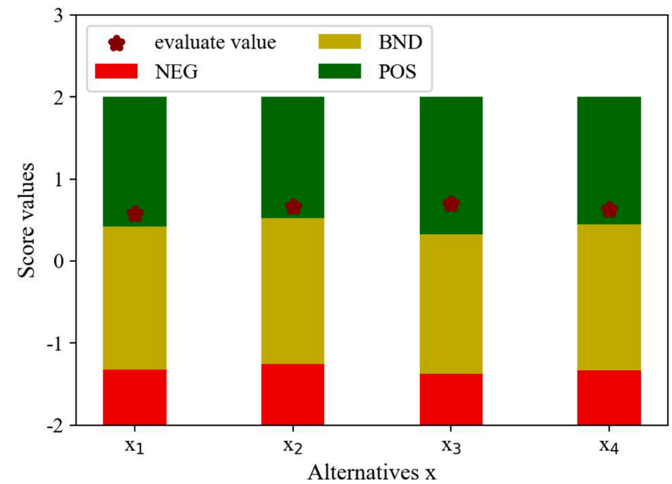

Fig. 5. The classification result in UDBSS instance.

Upon examination of the graph, it becomes evident that DM z_1 consistently attains the highest P-R value, irrespective of whether it is for α or β. Consequently, the thresholds associated with DM z_1 are chosen as the ultimate thresholds. In the final step, the definitive thresholds $\alpha_{j,final}$ and $\beta_{j,final}$ $(j = 1, 2, 3, 4)$ are derived, as outlined in Table 7.

(5) By employing Formulas (33) and (34), we proceed to compare the conclusive evaluation value with the ultimate threshold, yielding the Adjustable MG CIF PRSs. Additionally, with the assistance of Formulas (35) - (37), we can further segregate the outcome into three distinct regions, denoted as $POS^{\tau,\alpha_{j,final}}(X)$, $BND^{\tau,\alpha_{j,final},\beta_{j,final}}(X)$, and $NEG^{\tau,\beta_{j,final}}(X)$, which are non-adjacent to one another. The specific classification outcome for this case is visually depicted in Fig. 5.

From the above figure, we can see that all locations are divided into the domain $POS^{\tau,\alpha_{j,final}}(X)$, which reflect that all of the alternatives are likely to be locations that require the most bicycles.

(6) Within the confines of criterion $POS^{\tau,\alpha_{j,final}} \succ BND^{\tau,\alpha_{j,final},\beta_{j,final}} \succ NEG^{\tau,\beta_{j,final}}$, we initiate a ranking process for the ultimate evaluation values, applying the sorting criteria delineated in Definition 3.4. In Fig. 6, the score values for each location are graphically represented, enabling us to make a definitive determination, that is, $x_3 \succ x_2 \succ x_4 \succ x_1$. Then, it becomes evident that the optimal solution corresponds to location x_3 (H103).

Remark 6.2. Drawing from the comprehensive analysis conducted in the preceding six steps, it's evident that we have assumed a neutral stance with respect to all associated risks. As we arrive at the conclusive experimental outcomes, it becomes evident that the most optimal

Table 7
Final thresholds in the UDBSS instance.

	x_1	x_2	x_3	x_4
α	(0.6744, 0.52562, 0.3073, 0.47438)	(0.71673, 0.5393, 0.26763, 0.4607)	(0.48593, 0.66017, 0.48375, 0.33983)	(0.63299, 0.57932, 0.34608, 0.42068)
β	(0.20021, 0.12943, 0.785, 0.87057)	(0.22905, 0.13478, 0.75643, 0.86522)	(0.11316, 0.19311, 0.87216, 0.80689)	(0.17628, 0.15169, 0.80885, 0.84831)

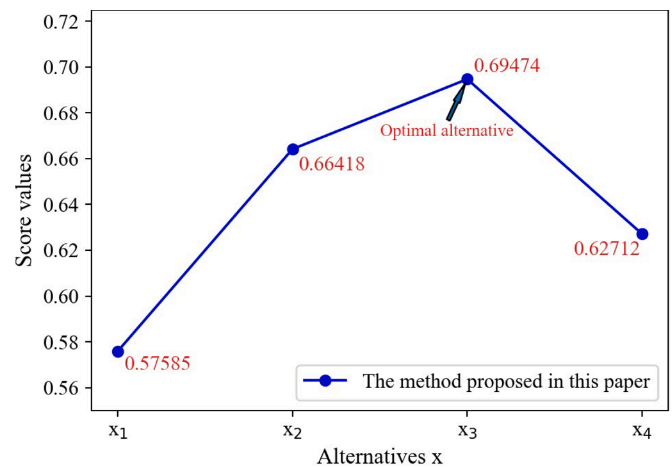

Fig. 6. The sorting result in UDBSS instance.

solution entails selecting location x_3. In other words, the prime location for the placement of a substantial number of urban shared bicycles is identified as H103. This is followed in order of preference by locations x_2(H102), x_4 (H105), and x_1 (H101). These results reveal the priorities of UDBSS for different locations when deploying shared bicycles.

6.3. Sensitivity analysis

To comprehensively investigate the influence of both parameter σ and parameter η on the outcomes generated by the model presented in this article, we have undertaken a parameter sensitivity analysis within this section. This analysis serves as an extension of the experiments conducted in Section 6.2 and allows us to gain a deeper understanding of how variations in these parameters impact the decision results.

(1) The integrated risk parameter of loss function is studied. We explore six distinct levels of attitudes towards risk, ranging from risk aversion to risk preference, with values of $\vartheta = 0.1$, $\vartheta = 0.2$, $\vartheta = 0.25$, $\vartheta = 0.3$, $\vartheta = 0.4$ and $\vartheta = 0.5$, respectively. When ϑ is equal to 0.1, due to the highest level of risk aversion, all four locations are divided into *BND*. As DMs exhibit a gradual shift towards a more risk-seeking attitude, the four locations are sequentially assigned to *POS*. Specifically, as ϑ exceeds a certain threshold, denoted by a $(0.2 < a < 0.25)$, all locations are divided

into *POS*. The experimental phenomenon described above is shown in Fig. 7.

The four locations are represented by different boxes. It is worth noting that beyond a certain point, the classification outcomes remain consistent. Therefore, in the figure, we have chosen to display only the initial four cases for clarity and brevity. The scoring values for each location are visually depicted using star symbols, and the classification results can be easily discerned by observing the specific range within which the star patterns are situated.

(2) We test the experimental phenomena under different values of η and the results are visualized, as shown in Fig. 8.

As we know, along with η increases, the risk also gradually increases. From this picture, we can observe that when there is a preference for risk avoidance, that is, $\eta = 1/4$ and $\eta = 2/4 = 1/2$, the optimal alternative is location x_1 (H101). At this point, the risk of choosing location x_1 is relatively small. But when there is a preference for accepting risk, that is $\eta = 3/4$ and $\eta = 4/4 = 1$, the optimal alternative is location x_3 (H103). At this time, choosing location x_3 will pose certain risks.

6.4. Comparative analysis

Building upon the outcomes obtained in the initial two sections, where we applied our model to derive sorting results for four distinct locations, this section aims to take our investigation a step further. To reinforce the credibility and efficacy of our model, we undertake a comparative analysis. In this analysis, we juxtapose our algorithm with several classical MG GMD methods that have been extended for use within the CIF environment. This comparative study enables us to meticulously analyze and discuss the disparities and distinctions among these approaches. Through this comprehensive examination, we aim to highlight the unique strengths and advantages offered by our model in contrast to established methodologies.

(1) The comparison with the CIF aggregation operator method

Our approach in this comparative analysis encompasses two distinct strategies. On one hand, we employ the CIF aggregation operator method (denoted as M1) to directly execute data fusion across both attribute and DM dimensions, culminating in the outcomes presented in Fig. 9. Next, we take a two-step approach. Initially, we utilize Definition 4.1 to acquire a single MG CIF information system. Subsequently, we apply the CIF aggregation operator method to execute data fusion

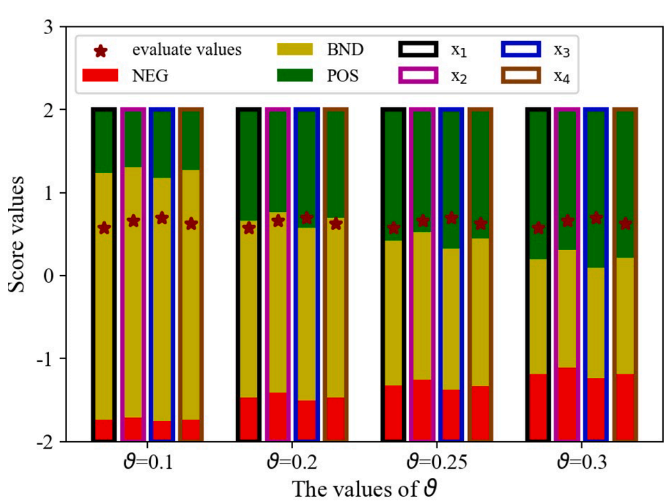

Fig. 7. The sensitivity analysis of parameter ϑ.

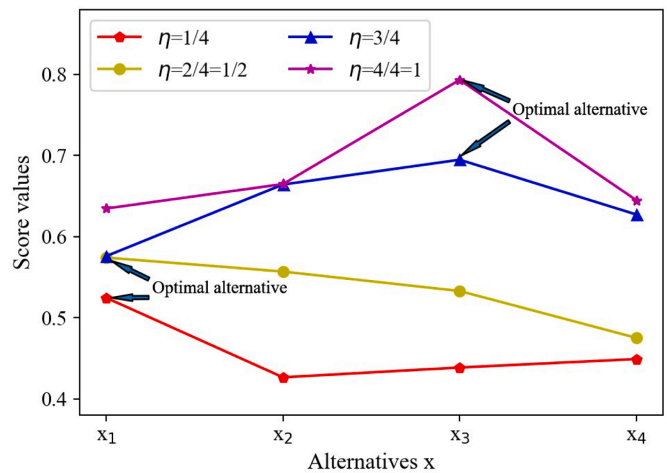

Fig. 8. The sensitivity analysis of parameter η.

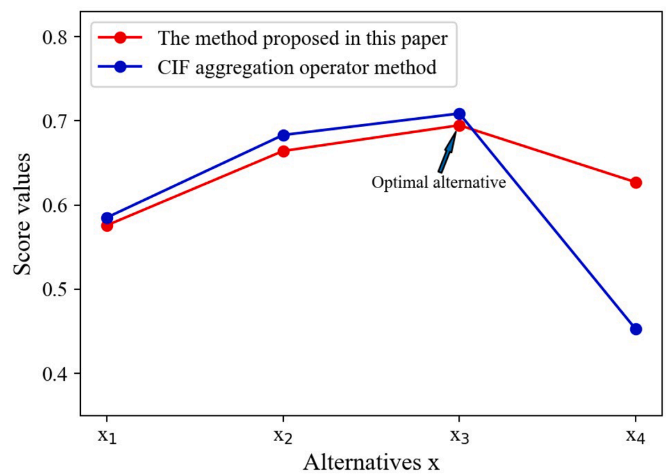

Fig. 9. The comparison with the CIF aggregation operator method.

exclusively within the DM dimension. This combined methodology is denoted as the TWD + CIF aggregation operator method (denoted as M2), and the outcomes are showcased in Fig. 10.

Based on the insights garnered from the two aforementioned graphs, a noteworthy observation emerges: our algorithm consistently aligns with the optimal location identified through the use of the aggregation

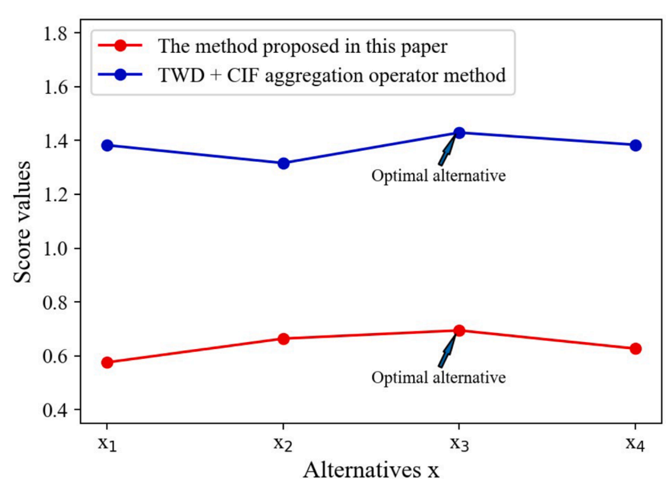

Fig. 10. The comparison with the TWD + CIF aggregation operator method.

operator method. This alignment underscores the reliability and effectiveness of our approach. Moreover, a deeper examination of Fig. 10 reveals an interesting phenomenon. By incorporating the TWD approach alongside the aggregation operator method, we observe a reduction in the impact of noisy data on the evaluation results. This reduction in noise-induced fluctuations signifies an improvement in the stability and robustness of our method. In summation, our approach not only showcases feasibility but also demonstrates superior stability when compared to established methodologies, ultimately enhancing its suitability for real-world applications.

(2) The comparison with the CIF TOPSIS method

In this section, we embark on a comparative analysis between our method and the CIF TOPSIS method (denoted as M3) and the approach known as TWD + CIF TOPSIS (denoted as M4). The CIF TOPSIS method is primarily centered on the computation of distances between each alternative and both the positive and negative ideal solutions. This computation allows us to discern the alternative that exhibits the highest degree of proximity to the positive ideal solution while simultaneously maintaining the lowest degree of closeness to the negative ideal solution, thereby identifying the optimal alternative. By applying this calculation, we yield the results displayed in Figs. 11 and 12.

The TOPSIS method relies on the calculation of distances from each solution to the positive and negative ideal solutions to establish their prioritization. Consequently, when a particular day at a specific location exhibits an exceptional volume of bicycle usage or returns, it can significantly skew the evaluation results for all solutions on that day. This skew can then propagate to influence the final ranking outcomes, as evidenced in the results depicted in Fig. 11. To address this issue comprehensively, we employ a two-step approach. Initially, we utilize Definition 4.1 to process the data, encompassing all dates, thereby mitigating the impact of exceptional dates. Subsequently, we apply the TOPSIS method to derive the final evaluation values, as showcased in Fig. 12. Remarkably, the results align with those obtained using our approach detailed in this article, demonstrating the efficacy of our method in managing the influence of exceptional data points.

(3) The comparison with the CIF VIKOR method

Similar to the preceding experiment, we undertake a comparative analysis, this time juxtaposing our algorithm with the CIF VIKOR method (denoted as M5) and the augmented TWD + CIF VIKOR method (denoted as M6). In these methodologies, the desirability of an alternative is indicated by lower evaluation values. For ease of interpretation, we transform the acquired evaluation values into benefit data. Let's

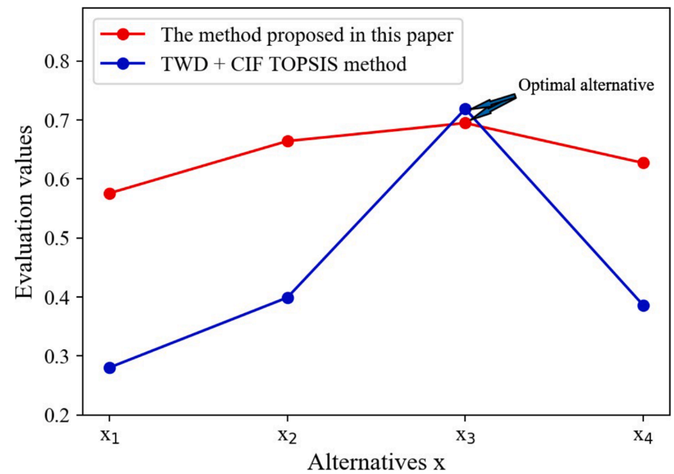

Fig. 12. The comparison with the TWD + CIF TOPSIS method.

assume the original evaluation value is represented as a. By applying a simple transformation, we derive the final evaluation value b, where $b = 1 - a$. This transformation enables us to present the results more intuitively, with lower values indicating more favorable alternatives. The outcomes of this analysis are elucidated in Fig. 13 and Fig. 14, shedding light on the relative performance of these approaches in evaluating and ranking alternatives.

The CIF VIKOR method builds upon the foundation of the CIF TOPSIS method, incorporating an additional layer of decision risk parameters. This augmentation allows DMs to exert influence on the decision results in accordance with their individual experiences, thereby introducing a degree of variability and adaptability into the decision outcomes. This enriched approach expands the range of potential decision results, accommodating the diverse perspectives and preferences of the DMs. In line with our experiment's adoption of a risk-neutral stance, the risk preference parameter is set at 0.5. Applying this parameter to the CIF VIKOR method, we arrive at the conclusion that the optimal alternative is location x_3 (H103).

(4) The comparison with the TWD + CIF regret theory method

In this section, we employ TWD + CIF regret theory (denoted as M7) to compute the regret value associated with each alternative. The evaluation value of a given alternative is derived through a comparison with the utility values of other available schemes. A higher evaluation value signifies a lower degree of regret associated with selecting the

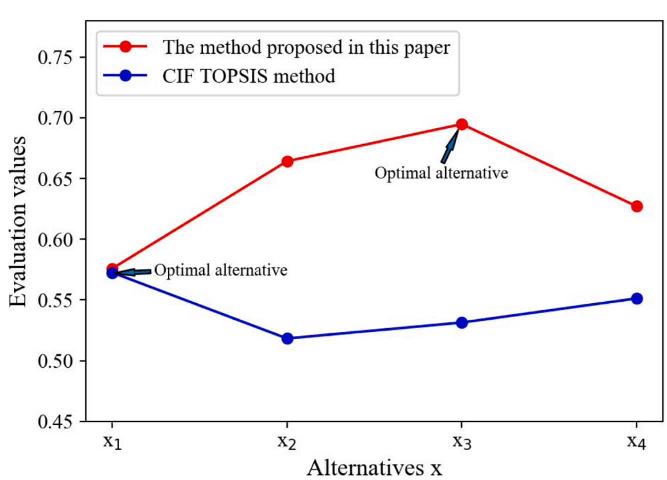

Fig. 11. The comparison with the CIF TOPSIS method.

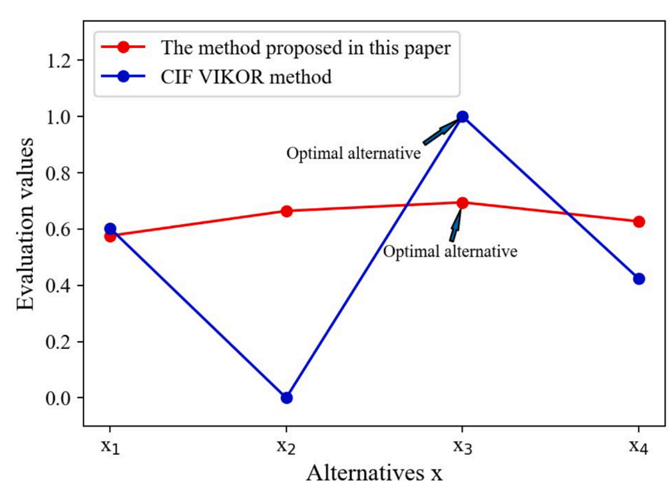

Fig. 13. The comparison with the CIF VIKOR method.

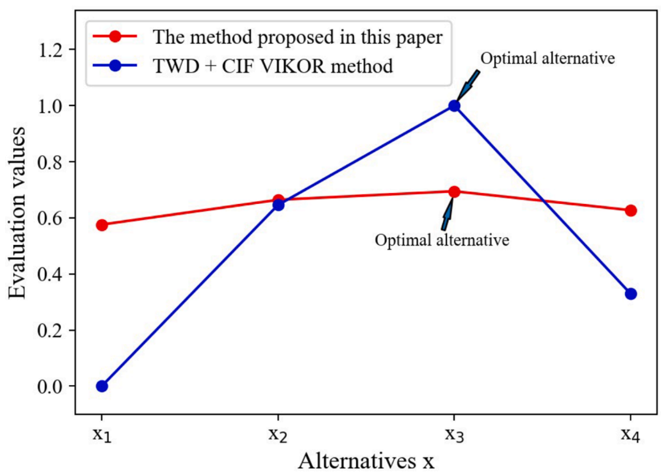

Fig. 14. The comparison with the TWD + CIF VIKOR method.

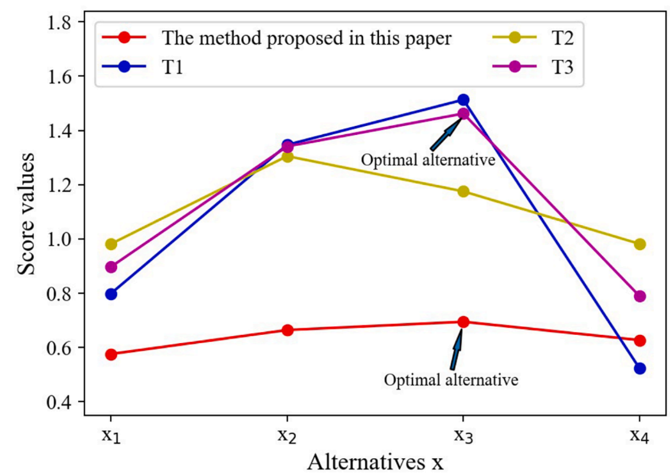

Fig. 16. Compare with literature (Zhang et al., 2019).

current alternative, as it indicates a more advantageous choice in comparison to the alternatives. The outcomes of this calculation are visually presented in Fig. 15. A noteworthy observation is that the optimal location obtained through the CIF regret theory align consistently with those derived from our method.

(5) The comparison with Literature (Zhang et al., 2019)

In our analysis, we conducted a comparative assessment between the method outlined in Literature (Zhang et al., 2019) (denoted as M8) and the approach detailed in this paper. The methodology described in Literature (Zhang et al., 2019) employs optimistic and pessimistic rough sets as metrics to formulate three distinct sets. Subsequently, it identifies the intersection among these sets as the optimal alternative. Upon examination of Fig. 16, it becomes evident that, based on this methodology, location x_3 (H103) emerges as the optimal selection. This finding serves as a valuable point of comparison, highlighting how our approach aligns or deviates from existing methods and shedding light on the unique contributions and advantages of our proposed methodology (denoted as M9).

6.5. Correlation analysis

In this section, we utilize the Spearman correlation coefficient to investigate the relationships between methods M1 to M9. This method allows us to obtain results as depicted in Fig. 17. By examining this figure, we gain insights into the degree of correlation between our proposed approach and methods M3, M4, M5, and M6. Notably, our method exhibits a relatively strong correlation with these specific methods. Conversely, its correlation with the remaining methods is somewhat weaker, albeit still concentrated around the 0.5 mark.

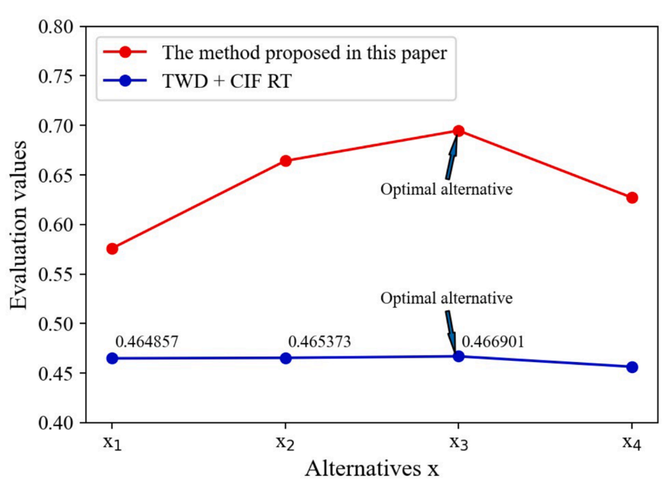

Fig. 15. The comparison with the TWD + CIF regret theory method

Remark 6.3. Through the comprehensive analysis presented above, we have conducted a series of comparative experiments involving these five methods. Furthermore, we have amalgamated some of these methods with Definition 4.1 to yield even more refined experimental results. Our objective is to provide a clearer illustration of the advantages inherent in our method when contrasted with classical methodologies. To facilitate this comparison, we have tabulated the distinctions among the various CIF MG GMD methods discussed herein, as outlined in Table 8. In summary, our approach exhibits superior performance in four key areas, underscoring its efficacy and utility compared to classical methods. These areas of superiority will be detailed and elaborated upon in the subsequent discussion.

7. Conclusions

As the third wave of the information technology industry continues to advance, coupled with the integration of data driven IoT, it becomes feasible to build a more intelligent, integrated, and efficient MITSs. Therefore, this paper addresses a pivotal component of the MITSs, namely the UDBSS, and proposes the rebalancing model for UDBSS. This model is of paramount importance for addressing the issue of unreasonable allocation in shared bicycles. This initiative not only offers significant advantages in terms of enhancing urban traffic flow, optimizing spatial resource utilization, and improving accessibility but also contributes to propelling cities toward a more sustainable development path. Nevertheless, UDBSS is an extremely complex decision-making environment. In this context, the present study has adopted an innovative approach, constructing a CIF decision matrix. Furthermore, to address the rebalancing problem for UDBSS effectively, the study has introduced the adjustable MG PRSs and P-RT, presenting a novel rebalancing model for UDBSS. The central objective of this model is to minimize unfulfilled resident demands by forecasting future vehicle usage patterns, thus achieving highly precise allocation of shared bicycles. Ultimately, we have applied this model to a real UDBSS data set and validated its exceptional performance through a series of experiments.

In terms of future research directions, we believe there should be a focus on the following aspects:

Fig. 17. The result of Spearman correlation coefficients from M1 to M9.

Table 8
The comparative analysis of advantages of different CIF MG GDM methods.

	Subjective opinions of experts	Bounded rationality	Stable results	Classification ability
M1	×	×	×	×
M2	×	×	√	√
M3	×	×	×	×
M4	×	×	√	√
M5	√	×	×	×
M6	√	×	√	√
M7	√	×	√	×
M8	×	×	√	×
M9	√	√	√	√

(1) In the real world, data incompleteness often occurs due to various factors. Therefore, it is necessary to study methods for complement incomplete data.
(2) Given the ever-expanding volume of data, data clustering to reduce data size is of paramount primary. Hence, it is crucial to explore differences among various clustering methods and foster innovation in this area.
(3) The issue of consistency in decision-making environments ids worth researching. There are two stages that can be explored separately: consistency discrimination and consistency achievement.

These research areas are critical to further improve the applicability of our method in the field of MITSs.

Data availability statement

The data that support the findings of this study are available from the corresponding author upon reasonable request Table.

CRediT authorship contribution statement

Chao Zhang: Methodology, Investigation, Writing – original draft. **Jiahui Zhang:** Conceptualization, Methodology, Writing – original draft. **Wentao Li:** Methodology, Investigation, Writing – original draft. **Oscar Castillo:** Methodology, Investigation. **Jiayi Zhang:** Methodology.

Declaration of Competing Interest

The authors declare that they have no known competing financial interests or personal relationships that could have appeared to influence the work reported in this paper.

APPENDIX

Table 9
The list of abbreviations.

Abbreviation	Meaning
UDBSS	Urban dockless bicycle sharing system
MG	Multi-granularity
CIF	Complex intuitionistic fuzzy
CIFSs	Complex intuitionistic fuzzy sets
TWD	Three-way decision
PRSs	Probability rough sets
DM	Decision-maker
PT	Prospect theory
RT	Regret theory
P-RT	Prospect-regret theory
MITSs	Modernized intelligent transportation systems
IoT	Internet of Things
GDM	Group decision-making
IFSs	Intuitionistic fuzzy sets
ND	Non-membership degrees
MD	Membership degrees
CFSs	Complex fuzzy sets
CIFN	Complex intuitionistic fuzzy number
CFN	Complex fuzzy number

Table 10
The list of main symbols.

Symbols	Meaning
C	CIFS
μ	MD
ρ	ND
r	Real part of MD
ω	Imaginary part of MD
k	Real part of ND
ϖ	Imaginary part of ND
γ	CIFN
U	Alternative set
x	Alternative
V	Attribute set
y	Attribute
u	Attribute weight
Z	DM set
z	DM
w	DM weight
R	Relation set
S	Standard assessment set
Sc	Score function
H	Accuracy function
d	Distance function
P	PRSs
τ	The risk parameter of the adjustable PRS
$\overline{\sum_{i=1}^{l} R_i}^{\tau,\beta_{j,final}}$	Upper approximation
$\underline{\sum_{i=1}^{l} R_i}^{\tau,\alpha_{j,final}}$	Lower approximation
τ	The risk parameter of the adjustable PRS
$POS^{\tau,\alpha_{j,final}}$	Positive region
$NEG^{\tau,\beta_{j,final}}$	Negative region
$BND^{\tau,\alpha_{j,final},\beta_{j,final}}$	Boundary region
$\alpha_{j,final}, \beta_{j,final}$	Final thresholds
σ	The risk parameter of the loss function
S	Standard assessment set
PRV	P-R value

References

Akram, M., Peng, X., & Sattar, A. (2021). A new decision-making model using complex intuitionistic fuzzy Hamacher aggregation operators. *Soft Computing, 25*, 7059–7086. https://doi.org/10.1007/s00500-021-05658-9

Alkouri, A. M. D. J. S., & Salleh, A. R. (2012). Complex intuitionistic fuzzy sets. *AIP Conference Proceedings, 1482*(1), 464. https://doi.org/10.1063/1.4757515

Atanassov, K. T. (1986). Intuitionistic fuzzy sets. *Fuzzy Sets and System, 20*(1), 78–96. https://doi.org/10.1016/S0165-0114(86)80034-3

Bell, D. E. (1982). Regret in decision making under uncertainty. *Operations Research, 30* (5), 961–981. http://www.jstor.org/stable/170353.

Bilotta, S., & Nesi, B. (2022). Estimating CO_2 Emissions from IoT Traffic Flow Sensors and Reconstruction. *Sensors-Basel, 22*(9), 3382. https://doi.org/10.3390/s22093382

Brinkmann, J., Ulmer, M. W., & Mattfeld, D. C. (2019). Dynamic lookahead policies for stochastic-dynamic inventory routing in bike sharing systems. *Computer and Operation Research, 106*, 260–279. https://doi.org/10.1016/j.cor.2018.06.004

Bulhões, T., et al. (2018). The static bike relocation problem with multiple vehicles and visits. *European Journal of Operational Research, 264*, 508–523. https://doi.org/10.1016/j.ejor.2017.06.028

Cai, Y., Ong, G. P., & Meng, Q. (2022). Dynamic bicycle relocation problem with broken bicycles. *Transportation Research Part E-Logistics and Transportation., 165*, Article 102877. https://doi.org/10.1016/j.tre.2022.102877

Cheng, S., Wu, Y., Li, Y., Yao, F., & Min, F. (2021). TWD-SFNN Three-way decisions with a single hidden layer feedforward neural network. *Information Sciences, 579*, 15–32. https://doi.org/10.1016/j.ins.2021.07.091

Dell'Amico, M., Iori, M., Novellani, S., & Stützle, T. (2016). A destroy and repair algorithm for the Bike sharing rebalancing problem. *Computer and Operation Research, 71*, 149–162. https://doi.org/10.1016/j.cor.2016.01.011

Deveci, M., Varouchakis, E. A., Brito-Parada, P. R., Mishra, A. R., & Rani, P. (2023). Evaluation of risks impeding sustainable mining using Fermatean fuzzy score function based SWARA method. *Applied Soft Computing, 139*, Article 110220. https://doi.org/10.1016/j.asoc.2023.110220

Eren, E., & Uz, V. E. (2020). A review on bike-sharing: The factors affecting bike-sharing demand. *Sustainable Cities and Society, 54*, Article 101882. https://doi.org/10.1016/j.scs.2019.101882

Gao, K., Li, A., Liu, Y., Gil, J., & Bie, Y. (2023). Unraveling the mode substitution of dockless bike-sharing systems and its determinants: A trip level data-driven interpretation. *Sustainable Cities and Society, 98*, Article 104820. https://doi.org/10.1016/j.scs.2023.104820

Garg, H., & Rani, D. (2019). A robust correlation coefficient measure of complex intuitionistic fuzzy sets and their applications in decision-making. *Applied Intelligence, 49*, 496–521. https://doi.org/10.1007/s10489-018-1290-3

Garg, H., & Rani, D. (2019). Some generalized complex intuitionistic fuzzy aggregation operators and their application to multicriteria decision-making process. *Arabic Journal for Science and . Engineering, 44*, 2679–2698. https://doi.org/10.1007/s13369-018-3413-x

Garg, H., & Rani, D. (2020). Novel aggregation operators and ranking method for complex intuitionistic fuzzy sets and their applications to decision-making process. *Artificial Intelligence Review, 53*, 3595–3620. https://doi.org/10.1007/s10462-019-09772-x

Garg, H., & Rani, D. (2020). Robust Averaging–Geometric Aggregation Operators for Complex Intuitionistic Fuzzy Sets and Their Applications to MCDM Process. Arab. *J. Sci. Eng., 45*, 2017–2033. https://doi.org/10.1007/s13369-019-03925-4

Garg, H., & Rani, D. (2020). Generalized geometric aggregation operators based on t-norm operations for complex intuitionistic fuzzy sets and their application to decision-making. *Cognative Computer., 12*, 679–698. https://doi.org/10.1007/s12559-019-09678-4

Gokasar, I., Pamucar, D., Deveci, M., Gupta, B. B., & Martinez, L. (2023). Metaverse integration alternatives of connected autonomous vehicles with self-powered sensors using fuzzy decision making model. *Information Science, 642*, Article 119192. https://doi.org/10.1016/j.ins.2023.119192

Gu, T., Kim, I., & Currie, G. (2019). To be or not to be dockless: Empirical analysis of dockless bikeshare development in China. *Transportation Research Part A: Policy and Practice, 119*, 122–147. https://doi.org/10.1016/j.tra.2018.11.007

Huang, G., & Xu, D. (2023). The last mile matters: Impact of dockless bike-sharing services on traffic congestion. *Transportation Research Part D: Transport and Environment, 121*, Article 103836. https://doi.org/10.1016/j.trd.2023.103836

Hussain, A., Ali, M. I., & Mahmood, T. (2020). Pythagorean fuzzy soft rough sets and their applications in decision-making. *Journal of Taibah University for Science, 14*(1), 101–113. https://doi.org/10.1080/16583655.2019.1708541

Jia, F., & Liu, P. (2019). A novel three-way decision model under multiple-criteria environment. *Information Sciences, 471*, 29–51. https://doi.org/10.1016/j.ins.2018.08.051

Kahnema, D., & Tversk, A. (1979). Prospect theory: An analysis of decision under risk. *Econometrica, 47*(2), 263–291. http://www.jstor.org/stable/1914185.
Li, W., & Xu, W. (2015). Double-quantitative decision-theoretic rough set. *Information Sciences, 316*, 54–67. https://doi.org/10.1016/j.ins.2015.04.020
Li, W., Xu, W., Zhang, H., & Zhang, J. (2022). Updating approximations with dynamic objects based on local multigranulation rough sets in ordered information systems. *Artificial Intelligence Review, 55*, 1821–1855. https://doi.org/10.1007/s10462-021-10053-9
Lin, M., Chen, Z., Liao, H., & Xu, Z. (2019). ELECTRE II method to deal with probabilistic linguistic term sets and its application to edge computing. *Nonlinear Dynamic, 96*, 2125–2143. https://doi.org/10.1007/s11071-019-04910-0
Lin, M., Huang, C., Chen, R., Fujita, H., & Wang, X. (2021). Directional correlation coefficient measures for Pythagorean fuzzy sets: Their applications to medical diagnosis and cluster analysis. *Complex and Intelligent System, 7*, 1025–1043. https://doi.org/10.1007/s40747-020-00261-1
Lin, M., Wang, H., Xu, Z., Yao, Z., & Huang, J. (2018). Clustering algorithms based on correlation coefficients for probabilistic linguistic term sets. *International Journal of Intelligent Systems, 33*, 2402–2424. https://doi.org/10.1002/int.22040
Liu, D., Li, T., & Ruan, D. (2011). Probabilistic model criteria with decision-theoretic rough sets. *Information Sciences, 181*, 3709–3722. https://doi.org/10.1016/j.ins.2011.04.039
Loomes, G., & Sugden, R. (1982). Regret theory: An alternative theory of rational choice under uncertainty. *Economic Journal, 92*(308), 805–824. http://www.jstor.org/stable/2232669.
Maleki, A., Nejati, E., Aghsami, A., & Jolai, F. (2023). Developing a supervised learning-based simulation method as a decision support tool for rebalancing problems in bike-sharing systems. *Expert Systems with Applications, 233*, Article 120983. https://doi.org/10.1016/j.eswa.2023.120983
Qian, Y., Liang, H., Lin, J., Guo, Q., & Liang, J. (2017). Local multigranulation decision-theoretic rough sets. *International Journal of Approximate Reasoning, 82*, 119–137. https://doi.org/10.1016/j.ijar.2016.12.008
Qian, Y., Liang, J., Yao, Y., & Dang, C. (2010). MGRS: A multi-granulation rough set. *Information Sciences, 180*, 949–970. https://doi.org/10.1016/j.ins.2009.11.023
Qian, Y., Zhang, H., Sang, Y., & Liang, J. (2014). Multigranulation decision-theoretic rough sets. *International Journal of Approximate Reasoning, 55*, 225–237. https://doi.org/10.1016/j.ijar.2013.03.004
Qiao, J., He, M., Sun, N., Sun, P., & Fan, Y. (2023). Factors affecting the final solution of the bike-sharing rebalancing problem under heuristic algorithms. *Computer and Operation Research, 159*, Article 106368. https://doi.org/10.1016/J.COR.2023.106368
Ramachandran, A., & Sangaiah, A. K. (2021). A review on object detection in unmanned aerial vehicle surveillance. *International Journal of Cognitive Computing in Engineering, 2*, 215–228. https://doi.org/10.1016/j.ijcce.2021.11.005
Ramot, D., Milo, R., Friedman, M., & Kandel, A. (2002). Complex fuzzy sets. *IEEE Transation of Fuzzy System, 10*(2), 171–186. https://doi.org/10.1109/91.995119
Rani, D., & Garg, H. (2017). Distance measures between the complex intuitionistic fuzzy sets and their applications to the decision-making process. *International Journal of Uncertainity Quantification, 7*(5), 423–439. https://doi.org/10.1615/Int.J.UncertaintyQuantification.2017020356
Sathiyaprasad, B. (2023). Ontology-based video retrieval using modified classification technique by learning in smart surveillance applications. *International Journal of Cognitive Computing in Engineering, 4*, 55–64. https://doi.org/10.1016/j.ijcce.2023.02.003
Thinh, T. N. H., Lam, P. M., Tran, H. Q., Tien, L. H. C., & Thai, P. H. (2023). Transformer vibration and noise monitoring system using internet of things. *Iet Communications, 17*, 815–828. https://doi.org/10.1049/cmu2.12585
Tian, Z., Zhou, J., Szeto, W. Y., Tian, L., & Zhang, W. (2020). The rebalancing of bike-sharing system under flow-type task window. *Transportation Research Part C: Emerging Technologies, 112*, 1–27. https://doi.org/10.1016/j.trc.2020.01.015
Torra, V. (2010). Hesitant fuzzy sets. *International Journal of Intelligent Systems, 25*(6), 529–539. https://doi.org/10.1002/int.20418
Wan, S., Zou, W., & Dong, J. (2020). Prospect theory based method for heterogeneous group decision making with hybrid truth degrees of alternative comparisons. *Computers & Industrial Engineering, 141*, Article 106285. https://doi.org/10.1016/j.cie.2020.106285
Wang, F., Gong, Z., & Shao, Y. (2022). Incomplete complex intuitionistic fuzzy system: Preference relations, expert weight determination, group decision-making and their calculation algorithms. *Axioms, 11*(8), 418. https://doi.org/10.3390/AXIOMS11080418
Wang, T., Li, H., Qian, Y., Huang, B., & Zhou, X. (2022). A regret-based three-way decision model under interval type-2 fuzzy environment. *IEEE Transation of Fuzzy System, 30*(1), 175–189. https://doi.org/10.1109/TFUZZ.2020.3033C448
Wang, T., Li, H., Zhou, X., Huang, B., & Zhu, H. (2020). A prospect theory-based three-way decision model. *Knowledge Based System, 103*, Article 106129. https://doi.org/10.1016/j.knosys.2020.106129
Wang, Y., Yang, Y., Wang, J., Douglas, M., & Su, D. (2021). Examining the influence of social norms on orderly parking behavior of dockless bike-sharing users. *Transportation Research Part A: Policty and Practice, 147*, 284–296. https://doi.org/10.1016/j.tra.2021.03.022
Wang, Z., & Ma, Y. (2022). Detection and recognition of stationary vehicles and seat belts in intelligent Internet of Things traffic management system. *Neural Computing Application, 34*, 3513–3522. https://doi.org/10.1007/s00521-021-05870-6
Xu, W., & Guo, Y. (2016). Generalized multigranulation double-quantitative decision-theoretic rough set. *Knowledge-Based System, 105*, 190–205. https://doi.org/10.1016/j.knosys.2016.05.021
Xu, X., et al. (2023). Exploring intra-urban human mobility and daily activity patterns from the lens of dockless bike-sharing: A case study of Beijing China. *International Journal of Applied Earth Observation, 122*, Article 103442. https://doi.org/10.1016/j.jag.2023.103442
Yao, Y. (2010). Three-way decisions with probabilistic rough sets. *Information Sciences, 180*, 341–353. https://doi.org/10.1016/j.ins.2009.09.021
Yao, Y. (2016). Three-way decisions and cognitive computing. *Cognative Computation, 8*, 543–554. https://doi.org/10.1007/s12559-016-9397-5
Yao, Y. (2018). Three-way decision and granular computing. *International Journal of Approximate Reasoning, 103*, 107–123. https://doi.org/10.1016/j.ijar.2018.09.005
Yao, Y. (2021). The geometry of three-way decision. *Applied Intelligence, 51*, 6298–6325. https://doi.org/10.1007/s10489-020-02142-z
You, P. (2019). A two-phase heuristic approach to the bike repositioning problem. *Applied Mathmatical Modelling, 73*, 651–667. https://doi.org/10.1016/j.apm.2019.04.030
Yu, H., Wang, X., Wang, G., & Zeng, X. (2020). An active three-way clustering method via low-rank matrices for multi-view data. *Information Sciences, 507*, 823–839. https://doi.org/10.1016/j.ins.2018.03.009
Zadeh, L. A. (1965). Fuzzy sets. *Infection Control, 8*, 338–353. https://doi.org/10.1016/S0019-9958(65)90241-X
Zhang, B., Li, X., & Saldanha-da-Gama, F. (2022). Free-floating bike-sharing systems: New repositioning rules, optimization models and solution algorithms. *Information Sciences, 600*, 239–262. https://doi.org/10.1016/j.ins.2022.03.028
Zhang, C., Li, D., & Liang, J. (2020). Multi-granularity three-way decisions with adjustable hesitant fuzzy linguistic multigranulation decision-theoretic rough sets over two universes. *Information Sciences, 507*, 665–683. https://doi.org/10.1016/j.ins.2019.01.033
Zhang, C., Li, D., Liang, J., & Wang, B. (2021). MAGDM-oriented dual hesitant fuzzy multigranulation probabilistic models based on MULTIMOORA. *International Journal of Machine Learning Cybernetics, 12*, 1219–1241. https://doi.org/10.1007/s13042-020-01230-3
Zhang, C., Li, D., Zhai, Y., & Yang, Y. (2019). Multigranulation rough set model in hesitant fuzzy information systems and its application in person-job fit. *International Journal of Machine Learning Cybernetics, 10*, 717–729. https://doi.org/10.1007/s13042-017-0753-x
Zhang, C., Zhang, J., Li, W., Pedrycz, W., & Li, D. (2023). A regret theory-based multi-granularity three-way decision model with incomplete T-spherical fuzzy information and its application in forest fire management. *Applied Soft Computing, 145*, Article 110539. https://doi.org/10.1016/j.asoc.2023.110539
Zhang, D., Xu, W., Ji, B., Li, S., & Liu, Y. (2020). An adaptive tabu search algorithm embedded with iterated local search and route elimination for the bike repositioning and recycling problem. *Computer and Operation Research, 123*, Article 105035. https://doi.org/10.1016/j.cor.2020.105035
Zhang, H., & Min, F. (2016). Three-way recommender systems based on random forests. *Knowledge Based System, 91*, 275–286. https://doi.org/10.1016/j.knosys.2015.06.019
Zhang, Y., & Mi, Z. (2018). Environmental benefits of bike sharing: A big data-based analysis. *Applied Energy, 220*, 296–301. https://doi.org/10.1016/j.apenergy.2018.03.101
Zhao, Y., Huang, X., Chen, N., Liu, H., & Huang, L. (2023). Integrated sensing and communication-promoted beam tracking and coverage for complex vehicular networks. *IET Communications, 17*, 1791–1805. https://doi.org/10.1049/cmu2.12654